LoL > PCA

Joshua T. Vogelstein, Minh Tang, Da Zheng, Randal Burns, Mauro Maggioni

Abstract

It is increasingly easy and common to acquire scientific data with hundreds, millions, or billions of predictors. The goal of is often to find a "discriminant boundary" that separates predictors into two classes (for example, healthy and diseased). Unfortunately, when the dimensionality of the predictors is larger than the sample size, there are an infinite number of equally good decision boundaries. To address this challenge researchers rely on dimensionality reduction techniques that search for a low-dimensional representations that preserve the discrimination information. Unfortunately, directly solving for the optimal low-dimensional representation for classification is computationally infeasible. Existing approaches either (i) modify the goal to find a low-dimensional representation that maximizes something else (such as Principal Components Analysis (PCA) or manifold learning to maximize variance), or (ii) make restrictive assumptions that require costly algorithms (such as Lasso to maximize sparsity). We therefore develop a method called "Linear Optimal Low-rank" embedding (LoL), by jointly utilizing both the directions of maximal variance (ignoring the classification task) and the direction of maximal discrimination (ignoring the variance). We show via a combination of theoretical results and simulations that LoL statistically dominates PCA and other linear methods under relatively general settings, meaning that no matter what the dimensionality of the original data, or the dimensionality of embedded data, or sample size, LoL finds a better representation of the data for subsequent classification, while adding negligible additional computational cost. Additional numerical experiments demonstrate that the same intuition may fruitfully be applied to hypothesis testing and regression. We demonstrate the performance of LoL as compared with existing standard methods on a genetics application, an image recognition application, and a connectomics application with over 500 million features comprising >400 gigabytes. In each case, LoL outperforms the other methods, while only requiring a few minutes on a single machine to run even on the huge dataset. Our open source implementation of LoL is easy to use, and computationally efficient, making it poised to tackle supervised dimensionality reduction challenges across disciplines.

Supervised learning—the art and science of estimating statistical relationships using labeled training data—is a crucial tool in scientific discovery. Supervised learning has been enabled a wide variety of basic and applied findings, ranging from discovering biomarkers in omics data [**?**] to object recognition from images [**?**]. A special case is classification; a classifier predicts the "class" of a novel observation via partitioning the space of observations (for example, predicting male or female from MRI scans). One of the most foundational and important approaches to classification is called "Fisher's Linear Discrimnant Analysis" (LDA) [1], which is based on very simple geometric reasoning. In particular, it is guaranteed to find the optimal linear classifier under the assumption that the data are Gaussian. Moreover, it can be applied no matter how many classes are present. Finally, its solution is analytic, therefore obviating costly numerical optimizations and enabling scalability. This solid theoretical foundation, easy interpretation, computational efficiency, and widespread utility perhaps contribute to LDA's longevity, as it remains one of the few reference classifiers nearly a century later.

Modern scientific datasets, however, present challenges for classification that were not addressed in Fisher's era. Specifically, the dimensionality of datasets is quickly ballooning. Currently, across many scientific disciplines, the raw data might consist of hundreds of millions of features or dimensions; for example, an entire genome or connectome. While the dimensionality of these data have increased precipitously, the sample sizes have not witnessed a concommitant increase. This "large p, small n" problem is disatrous for many classical statistical approaches because they were designed with "small p, large n" in mind. For example, LDA estimates a hyperplane in $p - 1$ dimensions when the data are p dimensional. But there are an infinite number of $p - 1$ dimensional hyperplanes that fit the data exactly when $p < n$. To see this, imagine fitting a line to a single point, or a plane to two points. In each case, one can choose any rotation, and still fit the data perfectly. Doing so, however, requires the algorithm to make a choice that is independent of the existing data, and therefore unlikely to be correct. This problem is typically called "over-fitting".

Many statistical and machine learning approaches have been developed to combat this over-fitting issue

when the dimensionality exceeds the sample size. Perhaps the most prominent strategy is to use principal components analysis (PCA) [?] to "pre-process" the data, that is, to reduce the dimensionality of the data prior to a subsequent classification using the much lower dimensional data. While hugely successful, PCA is a wholly *unsupervised* dimensionality reduction technique, meaning that PCA does not utilize the class labels while learning the low dimensional representation. A closely related approach for supervised learning is called "reduced-rank LDA" (RR-LDA). As we will show below, while PCA does not optimally utilize the class labels in its low-dimensional representation, RR-LDA actually *discards* this information.

A different strategy that focuses on utilizing the lable information is called "sparsity". Sparse methods find a small subset of the original features to use for subsequent inference [?]. There are many such approaches (often called "feature selection" or "feature screening"); the advantage of these approaches is that the result is sometimes more easily interpretable. The disadvantage, however, is that exactly solving the problem is computationally intractable, requiring time that is exponential in the number of features. That said, various approximations enable efficient algorithms that have provable guarantees under certain assumptions. LASSO is a particularly popular algorithm that has these properties. Unfortunately, LASSO still cannot run on millions of dimensions, and it has a hyper-parameter that requires careful tuning, and even then often produces spurious answers even when the unrealistically strict assumptions are met [?]. A more recent approach is called "regularized optimal affine discriminant" (ROAD). ROAD finds the optimal sparse dimensionaly reduction under certain gaussian assumptions. ROAD, however, can only be applied in two-class settings, and requires solving a computationally costly numerical optimization problem, and thus does not scale to large dimensionality.

Thus, analysts desire a method that has a simple geometric intuition even in high-dimensions and can be applied when there are any number of classes, but also has theoretical gurantees, without making addition assumptions about the data and requiring carefully tuning hyperparameters, and can scale to arbitrarily high-dimensional data in a computationally efficient fashion. To address these concerns, we developed "Linear Optimal Low-rank" embedding (LOL). The key intuition behind LOL is that we can jointly utilize both directions that are informative with regard to the classification task (the means) and the directions that maximize the variance (the covariance).

We demonstrate LOL outperforms—or at least performs no worse than—several reference benchmarks along every consideration mentioned above. This includes proving that LOL statistically dominates PCA and related linear methods under Gaussian assumption. Moreover, we provide an implementation that improves on previous computational capabilities in terms of stability and scalability. Numerical experiments quantitatively demonstrate the improvement of LOL over reference methods on a wide range of simulated experiments that satisfy our theoretical assumptions. By virtue of LOL being built upon geometric intuition, it is easy to extend it along various dimensions. Additional numerical experiments demonstrate that practice matches intuition, in particular, generalizations of LOL can easily be constructed to match different geometric assumptions of the data. Indeed, even when data are sampled from distributions outside our theory and intuition, LOL achieves smaller error than its competitors. In fact, one can extend this intuition outside of classification problems to other problems, including regression and hypothesis testing: a trivial modification of LOL leads to regression and testing procedures that also outperform the natural competitors. Computationally, LOL is always numerically stable, and requires no more computational space, and smaller computational time, than other linear methods. Moreover, we provide a highly scalable implementation that efficiently runs on terabyte datasets with hundreds of millions of features. Finally, we test LOL against a set of standard methods on four different benchmark real datasets. For any of the four different settings, there was not a single method that outperformed LOL in any dimension.

In addition to the above quantitative properties, LOL is intuitive, only has a single hyper-parameter which is exceedingly easy to tune, and we provide free and open source implementations, in MATLAB and R, as well as pre-configured environments that will enable anybody to run LOL on commodity machines, including laptops, workstations, and cloud instances. LOL is not likely to necessarily be the best algorithm on any given new high-dimensional challenge problem. Rather, we suspect LOL might be useful as one of the first algorithms to try on big and wide data. Moreover, the arguments and methodology developed herein provide a framework for developing big supervised manifold learning algorithms to tackle other data science challenges.
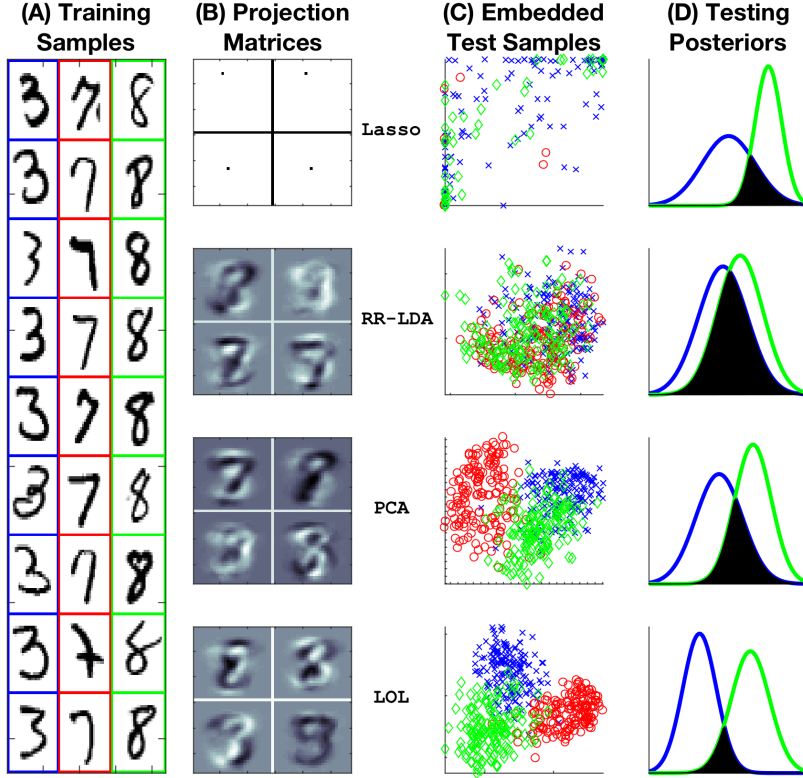
Figure 1: Illustrating four different classifiers—Lasso (top), LDA (second), PCA (third), and LoL (bottom)—for embedding images of the digits 3, 7, and 8 (from MNIST), each of which is $28 \times 28 = 784$ dimensional. **(A)** A subset of training samples (boundary colors are only for visualization purposes). **(B)** The first four projection matrices learned by the different approaches on 100 training samples from each class. Note that Lasso is sparse and supervised, PCAwhich is dense and unsupervised, and both LDA and LoL are dense and supervised. **(C)** Embedding 500 test samples into the top two dimensions using each approach. Digits color coded as in (A). **(D)** The estimated posterior distributions for 3 and 8 of test samples after projecting data into two dimensions via each method and using Lasso or LDA to classify. The filled area is the estimated error rate; the goal of any classification algorithm is to minimize that area. Clearly, LoL exhibits the best separation after embedding, which results in the best classification performance.

Results

An Illustrative Real Data Example of Supervised Linear Manifold Learning

A general strategy for high-dimensional classification proceeds as schematized in Figure 1: (A) obtain/select n training samples of the data, (B) learn a "linear projection map" from high-dimensions to low dimension, (C) project m testing samples onto the lower dimensional space, (D) classify the embedded testing samples using a linear classifier. We consider four different linear dimensionality reduction methods—Lasso, RR-LDA, PCA, and LoL—each of which we compose with a linear classifier to form high-dimensional classifiers. [1]

To demonstrate the utility of LoL, we first consider one of the most popular benchmark datasets ever, the MNIST dataset [3]. This dataset consists of $n = 60,000$ examples of images of the digits 0 through 9. Each such image is represented by a 28×28 matrix, which means that the observed (or ambient) dimensionality of the data is $p = 28^2 = 784$. Because we are motivated by the $n \ll p$ scenario, we subsample the data

---

[1]Although the original Lasso does not first find a low dimensional representation and then classify, more recent generalizations do (for exampel, **(author?)** [2]), and then improve on Lasso's theoretical and empirical properties, so will always mean Adaptive Lasso here.

89 to select $n = 300$ examples of the numbers 3, 7, and 8 (100 of each). We then apply all four approaches
90 to this subsample of the MNIST dataset, learning a projection, and embedding 500 testing samples, and
91 classifying the resulting embedded data.

92 LASSO, by virtue of being a sparse method, finds the pixels that most discriminate the 3 classes (column
93 B). The resulting embeddings mostly live along the boundaries (column C), because these images are
94 close to binary, and therefore, images either have or do not have a particular pixel. Indeed, although
95 the images themselves are nearly sparse (over 80% of the pixels in the dataset have intensity ≤ 0.05), a
96 low-dimensional discriminant boundary does not seem to be sparse, as evidenced by substantial overlap
97 between the posteriors for 3 and 8 (panel D).

98 RR-LDA does poorly, essentially failing to discriminate these digits at all. This is because the low dimen-
99 sional embedding implicit in RR-LDA subtracts out the difference of the means, only utilizing the dimensions
100 that maximize variance (see Appendix III.B for details). In this setting, it seems the directions that maxi-
101 mally separate the classes are not well aligned with the directions of maximal variance. On the other hand,
102 PCA does reasonably well, as it implicitly includes the discriminant directions merely by not subtracting them
103 out, but does not utilize them particularly well. LOL is our newly proposed supervised linear manifold learn-
104 ing method. The projection matrices it learns look qualitatively much like those of RR-LDA and PCA. This
105 is not surprising, as they are all linear combinations of the training examples. The resulting embeddings
106 however, look quite different. The three different classes are very clearly separated by even the first two
107 dimensions. The result of these embeddings yields classifiers whose performance is obvious from looking
108 at the embeddings: LOL achieves significantly smaller error than the other approaches (quantified by the
109 black area under the overlapping curves). This numerical experiment justifies the use of LOL, we next build
110 a geometric intuition for LOL in simple simulated examples, to better illustrate when we can expect LOL to
111 outperform other methods, and perhaps more importantly, when we expect LOL to fail.

Linear Gaussian Intuition

113 The above real data example suggests the geometric intuition for when LOL outperforms its sparse and un-
114 supervised counterparts. To further investigate, both theoretically and numerically, we consider the simplest
115 setting that illustrates the relevant geometry. In particular, we consider a two-class classification problem,
116 where both classes are distributed according to a multivariate normal distribution, where the two classes
117 have the same covariance matrix. so that the only difference between the classes is their means (we call
118 this the Linear Discriminant Analysis (LDA) model; see Methods for details).

119 Consider what the optimal projection would be in this scenario. The optimal low-dimensional projection is
120 analytically available as the dot product of the difference of means and the inverse covariance matrix, $\boldsymbol{A}_* =$
121 $\boldsymbol{\delta}^\mathsf{T} \boldsymbol{\Sigma}^{-1}$ [4] (see Methods for derivation). PCA, the dominant unsupervised manifold learning method, utilizes
122 only the covariance structure of the data, and ignores the difference between the means (because PCA for
123 classification operates on the class-conditionally centered data, see Methods for details). In particular,
124 PCA would project the data on the top d eigenvectors of the covariance matrix. **The key insight of our**
125 **work is the following: we can combine the difference of the means and the covariance matrix in a**
126 **simple fashion, rather than just the covariance matrix, to find a low dimensional projection.** Naïvely,
127 this should typically improve performance, because in this stylized scenario, both are important. The F2M
128 literature has a similar insight, but a different construction that requires the dimensionality to be smaller
129 than the sample size [5–9]. We implement our idea by simply concatenating the difference of the means
130 with the top d eigenvectors of the covariance matrix. This is equivalent to first projecting onto the difference
131 of the means vector, and then projecting the residuals onto the first d principle components. Thus, it
132 requires almost no additional computational time or complexity over that of PCA, rather, merely estimates
133 the difference of the means. In this sense, LOL can be thought of as a very simple "supervised PCA".

134 Figure 2 shows three different examples of data sampled from the LDA model to geometrically illustrate this
135 intuition. In each, we sample $n = 100$ training samples in $p = 1000$ dimensional space, so $n \ll p$. Figure 2A
136 shows an example we call "stacked cigars". In this example the covariance matrix is diagonal, so all ambient
137 dimensions are independent of one another. Moreover, the difference between the means and direction of
138 maximum variance are both large along the same dimensions (they are highly correlated with one another).
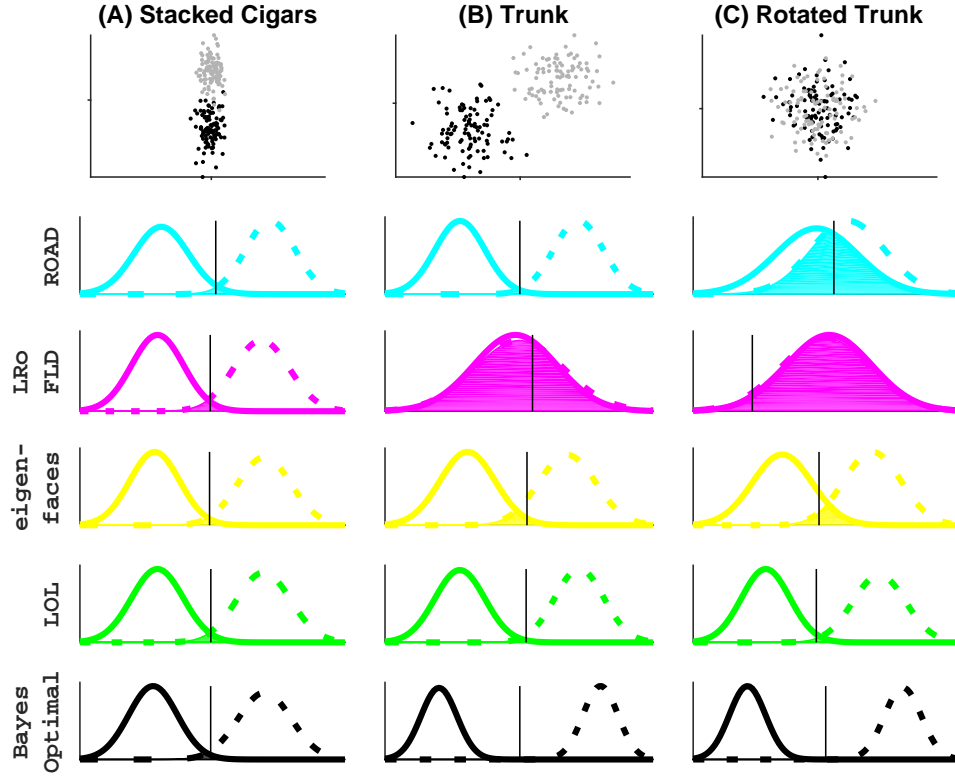
4

Figure 2: Lᴏʟ achieves near optimal performance for a wide variety of distributions. Each point is sampled from a multivariate Gaussian; the three columns correspond to different simulation parameters (see Methods for details). In each of 3 simulations, we sample $n = 100$ points in $p = 1000$ dimensions. And for each approach, we embed into the top 20 dimensions. Note that we use the sample estimates, rather than the true population values of the parameters. The five columns show (in decreasing order): **Row 1**: A scatter plot of the first two dimensions of the sampled points, with class 0 and 1 as black and gray dots, respectively. **Row 2** Fʟᴅ ∘ Pᴄᴀ. **Row 3** Rᴏᴀᴅ, a sparse method designed specifically for this model [10]. **Row 4** Lᴏʟ, our newly proposed method. **Row 5** the Bayes optimal classifier, which is what all classifiers strive to achieve. **(A)** The mean difference vector is aligned with the direction of maximal variance, maxing it ideal for both Pᴄᴀ to discover the discriminant direction and a sparse solution. In this setting, the results are similar for all methods, and essentially optimal. **(B)** The mean difference vector is orthogonal to the direction of maximal variance, making Pᴄᴀ fail, but sparse methods and Lᴏʟ can still recover the correct dimensions, achieving nearly optimal performance. **(C)** Same as B, but the data are rotated, in this case, only Lᴏʟ performs well. Note that Lᴏʟ is closest to Bayes optimal in all three settings.

This is an idealized setting for Pᴄᴀ, because Pᴄᴀ finds the direction of maximal variance, which happens to correspond to the direction of maximal separation. However, in the face of high-dimensional data, Pᴄᴀ does not weight the discriminant directions sufficiently, and therefore performs only moderately well.[2] Because all dimensions are independent, this is a good scenario for sparse methods. Indeed, Rᴏᴀᴅ, a sparse classifier designed for precisely this scenario, does an excellent job finding the most useful ambient dimensions. Lᴏʟ does the best of all three approaches, by using both the difference of the means and the covariance. This is obvious upon comparing each approach to the Bayes optimal solution for this setting, which is analytically available due to its simplicity.

Figure 2B shows an example which is a worst case scenario for using Pᴄᴀ to find the optimal projection for classification. In particular, the variance is getting larger for subsequent dimensions, $\sigma_1 < \sigma_2 < \cdots < \sigma_p$, while the magnitudes of the difference between the means are decreasing with dimension, $\delta_1 > \delta_2 < \cdots > \delta_p$. Thus, for any truncation level, Pᴄᴀ finds exactly the *wrong* directions. Rᴏᴀᴅ is not hampered by

---

[2]When having to estimate the eigenvector from the data, Pᴄᴀ performs even worse. This is because when $n \ll p$, Pᴄᴀ is an inconsistent estimator with large variance [11, 12].

this problem, it is also able to find the directions of maximal discrimination, rather than those of maximal variance. Again, LoL, by using both the means and the covariance, does extremely well.

Figure 2C is exactly the same as B, except the data have been randomly rotated in all 1000 dimensions. This means that none of the original coordinates have much information, rather, linear combinations of them do. This is evidenced by observing the scatter plot, which shows that the first two dimensions fail to disambiguate the two classes. PCA, being rotationally invariant, fails in this scenario as it did in B. Now, there is no small number of ambient dimensions that separate the data well, so ROAD also fails. LoL is unperturbed by this rotation; in particular, it is able to "unrotate" the data, to find dimensions that optimally separate the two classes.

Statistical Theory

The above numerical experiments provide the intuition to guide our theoretical developments.

Theorem 1. LoL *better than (or as good as)* PCA*, under the* LDA *model when the parameters are provided.*

In words, it is better to incorporate the mean difference vector into the projection matrix. The *degree* of improvement is a function of the embedding dimension d, the ambient dimensionality p, and the parameters (see Methods for details and proof), but the *existence* of an improvement, or at least no worse performance, is independent of those factors. Note that better here includes both bias and variance. In the population version of these two methods, there is no variance, so only the bias is important. Moreover, we know the conditions under which LoL is strictly better than PCA, they are formally stated in Assumption **??** (in Methods). Informally, LoL is better than PCA whenever the angle between the mean vector and the top d principal components is large enough. Under reasonable assumptions, in the appendix, we show that this happens 84% of the time.

Numerical Experiments Extending Our Theoretical Results

In the previous section, we proved that LoL is often better than PCA, and never worse under the LDA model, regardless of observed dimensionality, embedded dimensionality, and parameters, assuming the parameters are given. In this section, we numerically investigate what happens when the parameters must be estimated from training data, and in particular, from $n = 100$ training samples, when the observed dimensionality is $p = 100$. These results strengthen our theoretical results by providing exact magnitudes of performance, rather than merely better than guarantees, in addition to operating in a finite sample setting, more akin to real data scenarios.

LDA **Model** We begin by investigating three scenarios that satisfy the LDA model assumptions required by our proofs. First, consider the rotated trunk example from Figure 2C as well as a "Toeplitz" example, as depicted in Figures 3A and B, respectively. In both cases, we compare LoL to FLDoPCA and ROAD. In both scenarios, for all dimensions, LoL achieves a lower error rate than either of its competitors.

Multiple Classes LoL can trivially be extended to > 2 class situations. Naïvely it may seem like we would need to keep all pairwise differences between means. However, given k classes, the set of all k^2 differences is only rank $k - 1$. In other words, we can equivalently compute the distance of each mean to a single mean (in practice, for minimizing variance reasons, we use the class which has the maximum number of samples (breaking ties randomly). Figure 3C shows a 3-class generalization of the rotated Trunk example from Figure 3A. While LoL uses the additional class naturally, many previously proposed high-dimensional classifiers, such as ROAD, natively only work for 2-classes. Thus, we only compare LoL to FLDoPCA here. As before, LoL significantly outperforms FLDoPCA for all embedding dimensions.

Generalizations of LoL

The above simulations were all under the LDA model, for which we have theoretical guarantees that LoL should outperform FLDoPCA. In this section, we explore simulation settings that extend beyond the geometric constraints we required for our proofs, to develop an even deeper understanding of LoL.

Fat Tails Figure 3D shows a sparse example with "fat tails" to mirror real data settings better. More specifically, each class is the sum of multiple Gaussians, with the same mean, but different covariances (see Methods for details). The qualitative results are consistent with those of A and B, even though the setting is no longer exactly the setting under which we have theoretical confirmation. More specifically, LoL outperforms FLDoPCA and RoAD for all dimensions.

QDA Sometimes, it makes more sense to model each class as having a unique covariance matrix, rather than a shared covariance matrix. Assuming everything is Gaussian, the optimal classifier in this scenario is called Quadratic Discriminant Analysis (QDA) [13]. Intuitively then, we can modify LoL to compute the eigenvectors separately for each class, and concatenate them (sorting them according to their singular values). Moreover, rather than classifying the projected data with LDA, we can then classify the projected data with QDA. Indeed, simulating data according to such a model (Figure 3E), LoL performs slightly better than chance, regardless of the number of dimensions we use to project, whereas QOQ (for Quadratic Optimal QDA) performs significantly better regardless of how many dimensions it keeps. This demonstrates a straightforward generalization of LoL, available to us because of the simplicity and intuitiveness of LoL.

Outliers Outliers persist in many real data sets. Finding outliers, especially in high-dimensional data, is both tedious and difficult. Therefore, it is often advantageous to have estimators that are robust to certain kinds of outliers [14–16]. PCA and eigenvector computation are particularly sensitive to outliers [17]. Because LoL is so simple and modular, we can replace typical eigenvector computation with a robust variant thereof, such as the geometric median subspace embedding [18]. Figure 3F shows an example where we generated $n/2$ training samples according to the simple LDA model, but then added another $n/2$ training samples from a noise model. LRL (Linear Robust Low-Rank), performs better than LoL regardless of the number of dimensions we keep. This simulation setting further demonstrates the flexibility of the LoL framework to be extensible to other, more complicated scenarios.

XOR XOR is perhaps the simplest nonlinear problem, the problem that led to the demise of the perceptron, prior to its resurgence after the development of multi-layer perceptrons [19]. Thus, in our opinion, it is warranted to check whether any new classification method can perform well in this scenario. The classical (two-dimensional) XOR problem is quite simple: the output of a classifier is zero if both inputs are the same (00 or 11), and the output is one if the inputs differ (01 or 10). Figure 3G shows a high dimensional and stochastic variant of XOR (see Methods for details). This simulation was designed such that standard classifiers, such as support vector machines and random forests, achieve chance levels (not shown). LoL, performs moderately better than chance, and QOQ performs significantly better than chance, regardless of the chosen dimensionality. This demonstrates that our classifiers developed herein, though quite simple and intuition, can perform well even in settings where the data are badly modeled by our underlying assumptions. This mirrors previous findings where the so-called "idiots's Bayes" classifier outperforms more sophisticated classifiers [4]. In fact, we think of our work as finding intermediate points between idiot's Bayes (or naïve Bayes) and FLD, by enabling degrees of regularization by changing the dimensionality used.

Computational Efficiency

In many applications, the main quantifiable consideration in whether to use a particular method, other than accuracy, is computational efficiency. Because implementing LoL requires only highly optimized linear algebraic routines—including computing moments and singular value decomposition—rather than the costly iterative programming techniques currently required for sparse or dictionary learning type problems. Moreover, because LoL only requires computing means and covariances, we can leverage recent advances in parallel matrix operations [20] on fast solid-state drives (SSDs). We implement LoL with the R interface of FlashX [20–22]. Given the FlashX programming framework, we can run LoL on essentially arbitrarily large data. For these examples, we simulated data satisfying the LDA model; specifically, we used a spherically symmetric covariance matrix, with means just $\pm$ the one vector (see Methods for simulation details).

Figure 4A demonstrates both the in memory and semi-external memory [23] computing models of our implementation. For the in memory implementation (light green line), we see that the run time increases linearly with the number of dimensions, requiring about 11 minutes to run LoL on a $p = 32{,}000{,}000$ dimen-

7

sional problem with $n = 2000$ samples. This linear increase is the optimal scale up according to Ahmdel's Law [24]. This example already requires 477 gigabyte (GB) to store the data, but <1 GB to perform the computations. For larger data, we developed a semi-external memory implementation, which stores the data matrix on solid state drives, and the low-rank estimates in RAM [25]. This strategy allows us to run LoL as long as the data can fit on disk, and the low-rank approximation can fit in RAM. The semi-external memory implementation (dark green line) achieves the same performance as the in memory implementation whenever the data are small enough for in memory, and continues scaling optimally (linearly) as the dimensionality further increases to $p = 128,000,000$ dimensions, a multi-terabyte scenario.

Another option for making LoL scale up better is to utilize randomized algorithms. In particular, random projections—for which the data are multiplied by a lower-dimensional random matrix—have been shown to provide excellent approximation eigenvectors [26]. Moreover, very sparse random projections, in which the elements of the matrix are mostly zero, with ± 1 randomly distributed, have been shown to be effective, and have significant computational benefits [27]. We therefore further modified FlashX to incorporate random projections and very sparse random projections, and let LAL denote Linear Approximate Low-rank. Figure 4A shows an order of magnitude improvement in both the in-memory and semi-external memory implementations of LAL.

Figure 4B shows the error for LoL and FLDoPCA in this scenario, simply to demonstrate that even in this extremely high dimensional setting, LoL still outperforms FLDoPCA. As expected, LAL performs as well as LoL for the low dimensional settings.

Computational Theory

We reify the above computational experiments with theoretical statements. Computing the mean for each class requires $\mathcal{O}(n_j p)$ floating point operations (flops), where n_j is the number of samples per class. Subtracting the means requires $\mathcal{O}((J-1)p)$ flops, where J is the total number of classes. Computing the first d singular triples (left and right singular vectors, and singular value) requires $\mathcal{O}(npd)$ flops. The sparse random projection however only requires $\mathcal{O}(npd/c)$, where $c1$ is the sparsity of the sparse random projection matrix. Since, $d \ll n, p$, this can substantially reduce computational complexity. Regardless, LoL computation is clearly bottlenecked by the PCA computation or random projection for single threaded operations.

Our parallel in memory implementation scales-up optimally (linearly) with the number of threads, requiring $\mathcal{O}(npd/T)$ flops for LoL, and $\mathcal{O}(npd/cT)$ flops for LAL, where T is the number of threads. Our parallel semi-external memory implementation scales-out optimally (linearly) as well. This is in agreement with the linear fit of the lines in Figure 4A.

Benchmark Real Data Applications

Although LoL both statistically and computationally outperforms its natural competitors both in theory and in a variety of simulation settings, real data often tell a different story. We have therefore selected four commonly used high-dimensional datasets to compare LoL to several state-of-the-art algorithms (see Methods for details). For each dataset, we compare LoL to (i) support vector machines (SVM), (ii) ROAD, (iii) lasso, (iv) and random forest (RF). Because in practice all these approaches have "hyperparameters" to tune, we consider several possible values for SVM, lasso, and LoL (but not RF, as its runtime was too high). Figure 5 shows the results for all four datasets. For each, we use MATLAB implementations, partially because ROAD provides MATLAB code, and also because of MATLAB's ubiquity in certain communities. Because we also have R and FlashX implementations of LoL, comparisons using other languages would be straightforward.

Qualitatively, the results are similar across datasets: LoL achieves high accuracy and computational efficiency as compared to the other methodologies. Considering Figure 5A and B, two popular sparse settings, we find that LoL can find very low dimensional projections with very good accuracy. For the prostate data, with a sufficiently non-sparse solution for ROAD, it slightly outperforms LoL, but at substantial computational cost; in particular, ROAD takes about 100 times longer to run on this dataset. Figure 5C and D are 10-class problems, so ROAD is no longer possible. Here, SVM can again slightly outperform LoL, but again, requiring 100 fold additional computational time. In all cases, the beloved random forest classifier performs subpar.

294 In all four scenarios, there is never an algorithm that achieves smaller error in less time, as indicated by the
295 dark gray box being empty in the lower panels of Figure 5A-D.

Extensions to Other Supervised Learning Problems

297 The utility of incorporating the mean difference vector into supervised machine learning for big and wide
298 data extends beyond merely classification. In particular, hypothesis testing can be considered as a special
299 case of classification, with a particular loss function. Therefore we apply the same idea to a hypothesis
300 testing scenario. The multivariate generalization of the t-test, called Hotelling's Test, suffers from the same
301 problem as does the classification problem; namely, it requires inverting an estimate of the covariance matrix
302 whose estimate would be low-rank and therefore singular, in the high-dimensional setting. To mitigate this
303 issue in the hypothesis testing scenario, prior art applied similar tricks as they have done in the classification
304 setting. One particularly nice and related example is that of Lopes et al. [28], who addresses this dilemma
305 by using random projections to obtain a low-dimensional representation, following by applying Hotelling's
306 Test in the lower dimensional subspace. Figure 6A and B shows the power of their test alongside the power
307 of the same approach, but using the LoL projection rather than random projections. The two different
308 simulations include the simulated settings considered in their manuscript (see Methods for details). The
309 results make it clear that the LoL test has higher power for essentially all scenarios. Moreover, it is not
310 merely the replacing random projections with PCA (solid magenta line), nor simply incorporating the mean
311 difference vector (dashed green line), but rather, it appears that LoL for testing uses both modifications to
312 improve performance.

313 High-dimensional regression is another supervised learning method that can utilize the LoL idea. Linear
314 regression, like classification and Hotelling's Test, requires inverting a matrix as well. By projecting the
315 data only a lower dimensional subspace first, followed by linear regression on the low-dimensional data,
316 we can mitigate the curse of high-dimensions. To choose the projection matrix, we partition the data into K
317 partitions, based on the percentile of the target variable, we obtain a K class classification problem. Then,
318 we can apply LoL to learn the embedding. Figure 6C shows an example of this approach, contrasted with
319 LASSO and partial least squares, in a sparse simulation setting (see Methods for details). LoL is able to find
320 a better low-dimensional projection than LASSO, and performs significantly better than partial least squares,
321 for essentially all choices of number of dimensions to embed into.

Discussion

323 We have introduced a very simple, yet new, methodology to improve performance on supervised learning
324 problems with big and wide data. In particular, we have proposed a supervised manifold learning procedure
325 that utilizes both the difference of the means, and the covariance matrices, and proved that it performs better
326 than first applying PCA to the data under reasonable assumptions. This is in stark contrast to most previous
327 approaches, which only utilize the covariance matrices (or kernel variants thereof), or try to solve a difficult
328 optimization theoretic problem. In addition to demonstrating the statistical accuracy and computational
329 efficiency of LoL on simulated and real classification problems, we also demonstrate how the same idea
330 can also be used for other kinds of supervised learning problems, including regression and hypothesis
331 testing. Theoretical guarantees suggest that this line of research is promising and can be extended to other
332 more general settings and tasks.

333 **Related Work** One of the first publications to compose FLD with an unsupervised learning method was
334 the celebrated Fisherfaces paper [29]. The authors showed via a sequence of numerical experiments the
335 utility of embedding with PCA prior to classifying with FLD. We extend this work by adding a supervised
336 component to the initial embedding. Moreover, we provide the geometric intuition for why and when this
337 is advantageous, as well as show numerous examples demonstrating its superiority. We also prove that
338 Fisherfaces can be implemented very efficiently (see Methods), while shedding light on why it is performing
339 relatively well in general.

340 **Next Steps** The LoL idea, appending the mean difference vector to convert unsupervised manifold learning

to supervised manifold learning, has many potential applications. We have presented the first few. Incorporating additional nonlinearities via kernel methods [30], ensemble methods such as random forests [31], and multiscale methods [32] are all of immediate interest. MATLAB, R, and FlashR code for the experiments performed in this manuscript is available from http://docs.neurodata.io/LOL/.
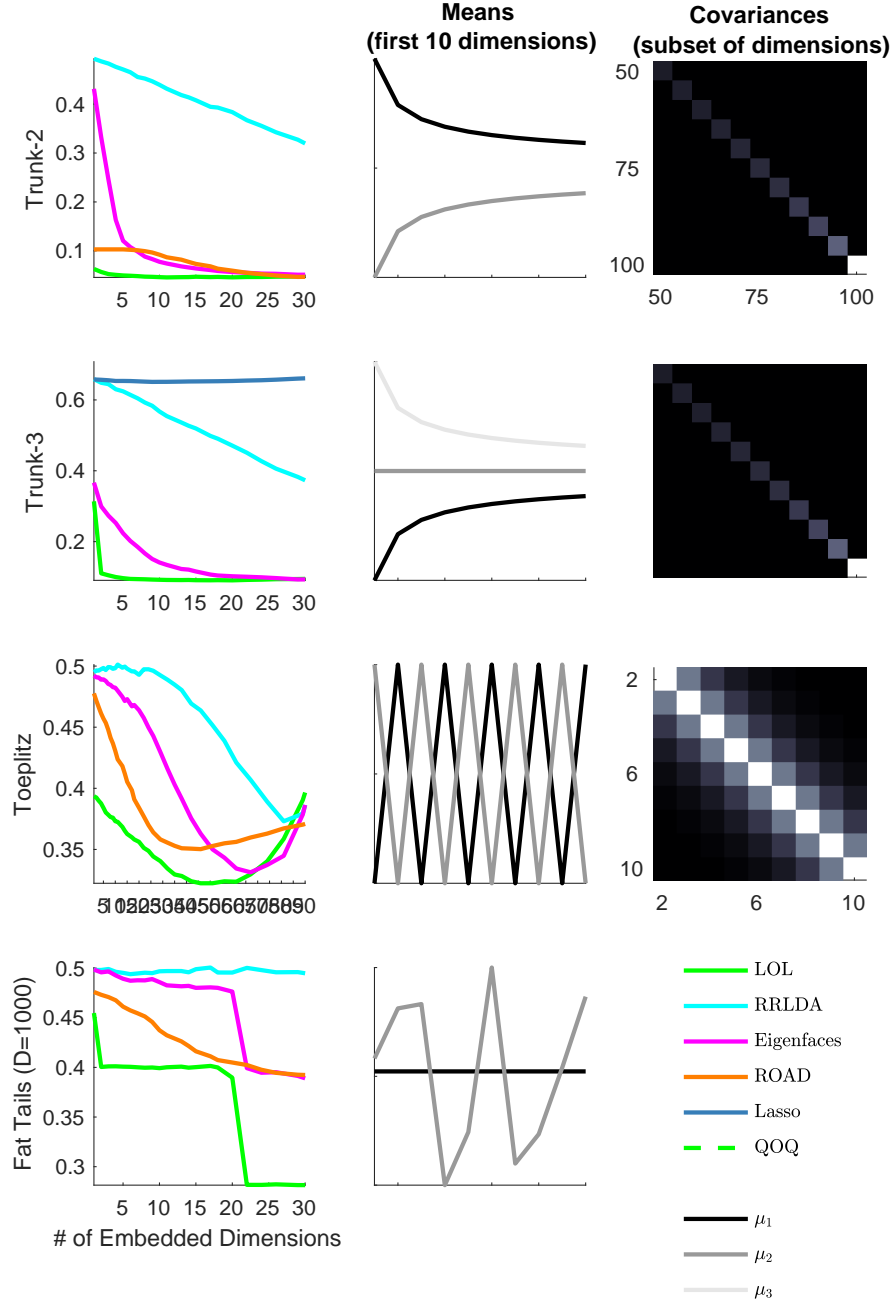
Figure 3: Seven simulations demonstrating `LOL` achieves superior finite sample performance over competitors both in settings for which we have asymptotic theoretical guarantees, and those for which we do not. For the first three, the top panels depict the means (top), the shared covariance matrix (middle). For the next three, the top panels depict a 2D scatter plot (left), mean and level set of one standard deviation of covariance matrix (right). For all seven simulations, the bottom panel shows misclassification rate as a function of the number of embedded dimensions, for several different classifiers. The simulations settings are as follows: **(A)** Rotated Trunk: same as Figure 2C. **(B)** Toeplitz: another setting where mean difference is not well correlated with any eigenvector, and no ambient coordinate is particularly useful on its own. **(C)** 3 Class variant of the rotated Trunk example to demonstrate that `LOL` naturally adapts, and excels in, multi-class problems. **(D)** Fat Tails: a common phenomenon in real data that is more general than our theory supports. **(E)** QDA: `QOQ`, a variant of `LOL` when each class has a unique covariance, outperforms `LOL`, as expected, when the true discriminant boundary is a quadratic, rather than linear, function. **(F)** Outliers: adding high-dimensional outliers degrades performance of standard eigensolvers, but those can easily be replaced in `LOL` for a robust variants (called `LRL`). **(G)** XOR: a high-dimensional stochastic generalization of XOR, demonstrating that `QOQ` works even in scenarios that are quite distinct from the original motivating problems. In all 7 cases, `LOL`, or the appropriate generalization thereof, outperforms unsupervised or sparse methods. Moreover, the optimal embedding dimension is never the true discriminant dimension, but rather, a smaller number jointly determined by parameter settings and sample size.
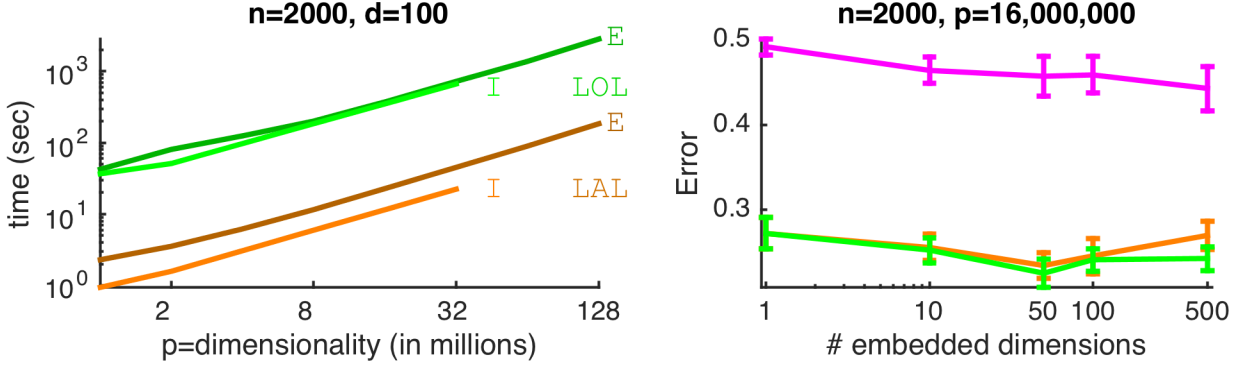
Figure 4: Computational efficiency of various low-dimensional projection methods. In all cases, $n = 2000$, and we used spherically symmetric simulation parameters (see Methods for details). We compare `PCA` with the projection step of `LOL` (light green for in memory, dark green for semi-external memory) and `LFL` (light orange for in-memory, dark orange for semi-external memory) for different observed dimensions (p). **(A)** `LOL` exhibits optimal (linear) scale up and scale out, requiring only 46 minutes to find the embedding on a 2TB dataset, and only 3 minutes using `LAL`(the sparse constant of sparse random projection $c = \dfrac{1}{\sqrt{p}}$). **(B)** Error for `LAL` is the same as `LOL` in this setting, and both are significantly better than `FLDoPCA` for all choices of embedding dimension.
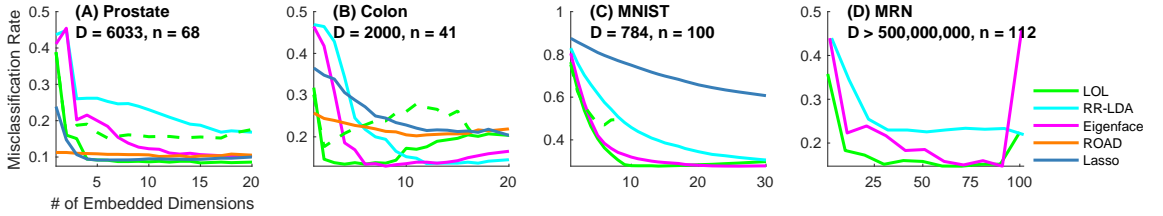
Figure 5: For four standard datasets, we benchmark `LOL` (green circles) versus standard classification methods, including support vector machines (blue up triangles), `ROAD` (cyan down triangles), `LASSO` (magenta pluses), and random forest (orange diamonds). Top panels show error rate as a function of $\log_2$ number of embedded dimensions (for `LOL`, `ROAD`, and `LASSO`) or cost (for SVM). Bottom panels show the minimum error rate achieved by each of the five algorithms versus time. The lower left dark gray (upper right light gray) rectangle is the area in which any algorithm is *better* (worse) than `LOL` in terms of both accuracy and efficiency. **(A)** Prostate: a standard sparse dataset. 1-dimensional `LOL` does very well, although keeping 2^5 ambient coordinates slightly improves performance, at a significant cost of compute time (two orders of magnitude), with minimal additional interpretability. **(B)** Colon: another standard sparse dataset. Here, 2-4 dimensions of `LOL` outperforms all other approaches considered regardless of how many dimensions they keep. **(C)** MNIST: 10 image categories, so `ROAD` is not possible. `LOL` does very well regardless of the number of dimensions kept. SVN marginally improves on `LOL` accuracy, at a significant cost in computation (two orders of magnitude). **(D)** CIFAR-10: a higher dimensional and newer 10 category image classification problem. Results are qualitatively similar to C. Note that, for all four of the problems, there is no algorithmperforming better and faster than `LOL`; rather, most algorithms typically perform worse and slower (though some are more accurate and much more computationally expensive).

(A) Diagonal
D=200, n=100

(B) Dense
D=200, n=100

(C) Sparse Toeplitz
D=1000, n=100

testing power

decay rate

decay rate

regression error

# of embedded dimensions

LOL
LAL
H o RP
H o PCA
Lasso
PLS
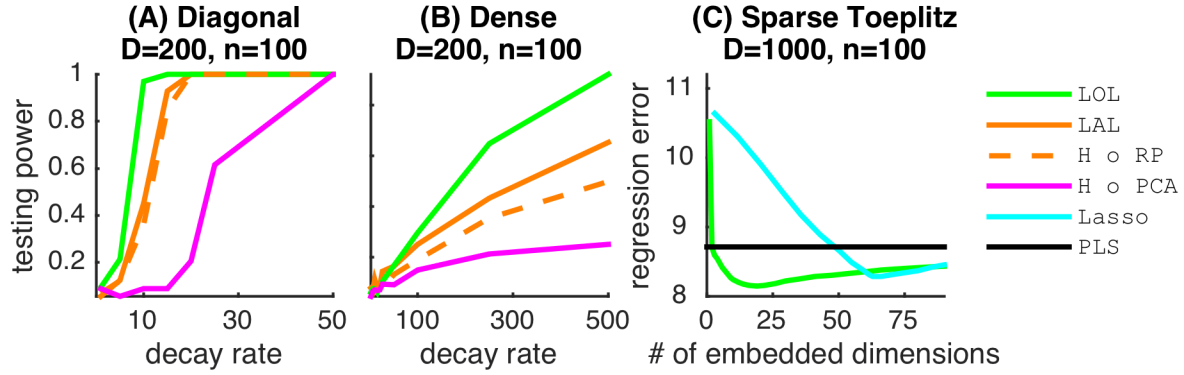
Figure 6: The intuition of including the mean difference vector is equally useful for other supervised manifold learning problems, including testing and regression. **(A)** and **(B)** show two different high-dimensional testing settings, as described in Methods. Power is plotted against the decay rate of the spectrum, which approximates the effective number of dimensions. LoL composed with Hotelling's test outperforms the random projections variants described in [28], as well as several other variants. **(C)** A sparse high-dimensional regression setting, as described in Methods, designed for sparse methods to perform well. Log_{10} mean squared error is plotted against the number of embedded dimensions. LoL composed with linear regression outperforms Lasso (cyan), the classic sparse regression method, as well as partial least squares (PLS; black). These three simulation settings therefore demonstrate the generality of this technique.

A Simulations

For most simulation settings, each class is Guassian: $f_{x|y} = \mathcal{N}(\boldsymbol{\mu}_y, \boldsymbol{\Sigma}_y)$, $f_y = \mathcal{B}(\pi)$. We typically assume that both classes are equally like, $\pi = 0.5$, and the covariance matrices are the same, $\boldsymbol{\Sigma}_0 = \boldsymbol{\Sigma}_1 = \boldsymbol{\Sigma}$. Under such assumptions, we merely specify $\boldsymbol{\theta} = \{\boldsymbol{\mu}_0, \boldsymbol{\mu}_1, \boldsymbol{\Sigma}\}$.

Stacked Cigars

- $\boldsymbol{\mu}_0 = \mathbf{0}$,
- $\boldsymbol{\mu}_1 = (a, b, a, \ldots, a)$,
- $\boldsymbol{\Sigma}$ is a diagonal matrix, with diagonal vector, $\boldsymbol{d} = (1, b, 1 \ldots, 1)$,

where $a = 0.15$ and $b = 4$.

Trunk

- $\boldsymbol{\mu}_0 = b/\sqrt{(1, 3, 5, \ldots, 2p)}$,
- $\boldsymbol{\mu}_1 = -\boldsymbol{\mu}_0$,
- $\boldsymbol{\Sigma}$ is a diagonal matrix, with diagonal vector, $\boldsymbol{d} = 100/\sqrt{(p, p-1, p-2, \ldots, 1)}$,

where $b = 4$.

Rotated Trunk

Same as Trunk, but the data are randomly rotated, that is, we sample $\boldsymbol{Q}$ uniformly from the set of p-dimensional rotation matrices, and then set:

- $\boldsymbol{\mu}_0 \leftarrow \boldsymbol{Q}\boldsymbol{\mu}_0$,
- $\boldsymbol{\mu}_1 \leftarrow \boldsymbol{Q}\boldsymbol{\mu}_1$,
- $\boldsymbol{\Sigma} \leftarrow \boldsymbol{Q}\boldsymbol{\Sigma}\boldsymbol{Q}^\mathsf{T}$.

Toeplitz

- $\boldsymbol{\mu}_0 = b \times (1, -1, 1, -1, \ldots, 1)$,
- $\boldsymbol{\mu}_1 = -\boldsymbol{\mu}_0$,
- $\boldsymbol{\Sigma}$ is a Toeplitz matrix, where the top row is $\rho^{(0, 1, 2, \ldots, p-1)}$,

where b is a function of the Toeplitz matrix such that the noise stays constant as dimensionality increases, and $\rho = 0.5$.

3 Classes

Same as Trunk, but with a third mean equal to the zero vector, $\mu_2 = \mathbf{0}$.

Fat Tails

For this setting, each class is actually a mixture of two Gaussians with the same mean (the two classes have the same covariances):

- $\boldsymbol{\mu}_0 = \mathbf{0}$,
- $\boldsymbol{\mu}_1 = (0, \ldots, 0, 1, \ldots, 1)$, where the first $s = 10$ elements are zero,
- $\boldsymbol{\Sigma}_0$ is a matrix with one's on the diagonal, and 0.2 on the off diagonal,
- $\boldsymbol{\Sigma}_1 = 15 \times \boldsymbol{\Sigma}_0$,

and then we randomly rotated as in the rotated Trunk example.

A. SIMULATIONS

QDA

A generalization of the Toeplitz setting, where the two classes have two different covariance matrices, meaning that the optimal discriminant boundary is quadratic.

- $\boldsymbol{\mu}_0 = b \times (1, -1, 1, -1, \ldots, 1)$,
- $\boldsymbol{\mu}_1 = -\boldsymbol{Q} \times (\boldsymbol{\mu}_0 + 0.1)$,
- $\boldsymbol{\Sigma}_0$ is the same Toeplitz matrix as described above, and
- $\boldsymbol{\Sigma}_1 = \boldsymbol{Q}\boldsymbol{\Sigma}_0\boldsymbol{Q}^\mathsf{T}$.

Outliers

In this dataset, we generate $n/2$ samples from an inlier model, and the remaining $n/2$ samples from an outlier model. For the inlier model, we first generate a random $d \times p$ dimensional orthonormal matrix, V, where $d = p/10$. Then, the first half of the inlier points are generated by $f_{x|0}$, the next half by $f_{x|1}$, and the remaining points generated by $f_{x|\emptyset}$. For the outliers, we sampled their class randomly from a fair Bernoulli distribution:

- $f_{x|0} = \mathcal{N}_d(0, \sigma^2) \times V^\mathsf{T}$,
- $f_{x|1} = \mathcal{N}_d(0, \sigma^2) \times V^\mathsf{T} + b$,
- $f_{x|\emptyset} = \mathcal{N}_p(\mathbf{0}, \sigma^2 \boldsymbol{I})$,
- $f_\emptyset = \mathcal{B}(0.5)$.

where we set $\sigma = 0.1$ and $b = 0.5$.

15

ALGORITHMS	p < n	2-Class LDA MODELS, p > n			GENERALIZED MODELS, p > n					OTHER TASKS, p > n		ALGORITHM PROPERTIES							ALGORITHMS	REF	NOTES
	LDA model	delta & cov aligned	& cov misaligned	delta & cov misaligned rotated	Fat Tails	>2 Class	QDA Model	Outlier Model	Non-linear	Testing	Regress	Fast	Simple	Theory	Open Source	Dense	2-step/ DL	Super-vised			
kNN	X	X	X	X	X	X		X	X		X		X	X	X	X		X	kNN	1	not considered
HCT	X	X	X									X	X	X			X	X	HCT	14	
LDA o Trace-Ratio	X	X	X	X								X	X	X		X	X	X	LDA o Trace-Ratio	4	
F2M / SDR	X			X		X							X	X	X	X	X	X	F2M / SDR	10	needs n>p
Deep Learning	X				X	X	X	X	X		X			X	X	X	X	X	Deep Learning	11	best when n>>p
Vowpal Wabbit	X				X	X		X			X	X			X	X	X	X	Vowpal Wabbit	5	best when n>>p
Ridge Regression	X											X	X	X	X	X		X	Ridge Regression	1	regression
Partial Least Squares											X	X						X	Partial Least Squares	1	regression
Naive Bayes	X	X	X			X						X	X	X	X	X		X	Naive Bayes	1,12	
HDDA	X	X	X	X		X								X	X			X	HDDA	6	
ROAD	X	X			X								X	X	X			X	ROAD	7,8,9	
LASSO	X	X				X					X	X	X	X	X		X	X	LASSO	3	
kSVM	X	X	X	X	X	X	X	X	X				X	X	X			X	kSVM	1	
Random Forest	X												X	X	X			X	Random Forest	1, 15	
LDA	X											X	X	X	X			X	LDA	1	
LDA o PCA	X	X				X					X	X	X	X	X	X	X	1/2	LDA o PCA	2	
LOL	X	X	X	X	X	X	X	X	X	X	X	X	X	X	X	X	X	X	LOL	*	
FIGURE		2A	2B, 3A	2C, 3B	3C	3D	3E	3F	3G	5A, 5D	5C, 5D	6									

Figure 7: Table of algorithms and their properties for high-dimensional data. Gray elements indicate that results are demonstrated in the Figure labeled in the bottom row. 'X' denotes relatively good performance for a given setting, or has the particular property.

B Theoretical Background

II.A The Classification Problem

Let $(\boldsymbol{X}, Y)$ be a pair of random variables, jointly sampled from $F := F_{\boldsymbol{X},Y} = F_{\boldsymbol{X}|Y}F_Y$. Let $\boldsymbol{X}$ be a multivariate vector-valued random variable, such that its realizations live in p dimensional Euclidean space, $\boldsymbol{x} \in \mathbb{R}^p$. Let Y be a categorical random variable, whose realizations are discrete, $y \in \{0, 1, \ldots C\}$. The goal of a classification problem is to find a function $g(\boldsymbol{x})$ such that its output tends to be the true class label y:

$$g^*(\boldsymbol{x}) := \underset{g \in \mathcal{G}}{\operatorname{argmax}} \mathbb{P}[g(\boldsymbol{x}) = y].$$

When the joint distribution of the data is known, then the Bayes optimal solution is:

$$g^*(\boldsymbol{x}) := \underset{y}{\operatorname{argmax}} f_{y|\boldsymbol{x}} = \underset{y}{\operatorname{argmax}} f_{\boldsymbol{x}|y}f_y = \underset{y}{\operatorname{argmax}}\{\log f_{\boldsymbol{x}|y} + \log f_y\} \tag{1}$$

Denote expected misclassification rate of classifier g for a given joint distribution F,

$$L_g^F := \mathbb{E}[g(\boldsymbol{x}) \neq y] := \int \mathbb{P}[g(\boldsymbol{x}) \neq y] f_{\boldsymbol{x},y} d\boldsymbol{x} dy,$$

where $\mathbb{E}$ is the expectation, which in this case, is with respect to F_{XY}. For brevity, we often simply write L_g, and we define $L_* := L_{g^*}$.

II.B Linear Discriminant Analysis (Lda)

Linear Discriminant Analysis (Lda) is an approach to classification that uses a linear function of the first two moments of the distribution of the data. More specifically, let $\mu_j = \mathbb{E}[F_{X|Y=j}]$ denote the class conditional mean, and let $\boldsymbol{\Sigma} = \mathbb{E}[F_X^2]$ denote the joint covariance matrix, and $\pi_j = \mathbb{P}[Y = j]$. Using this notation, we can define the Lda classifier:

$$g_{\text{Lda}}(\boldsymbol{x}) := \underset{y}{\operatorname{argmin}} \frac{1}{2}(\boldsymbol{x} - \boldsymbol{\mu}_0)^\mathsf{T}\boldsymbol{\Sigma}^{-1}(\boldsymbol{x} - \boldsymbol{\mu}_0) + \mathbb{I}\{Y = y\}\log \pi_y,$$

where $\mathbb{I}\{\cdot\}$ is one when its argument is true, and zero otherwise. Let L_{Lda}^F be the misclassification rate of the above classifier for distribution F. Assuming equal class prior and centered means, $\pi_0 = \pi_1$ and $(\boldsymbol{\mu}_0 + \boldsymbol{\mu}1)/2 = \boldsymbol{0}$, re-arranging a bit, we obtain

$$g_{\text{Lda}}(\boldsymbol{x}) := \underset{y}{\operatorname{argmin}} \boldsymbol{x}^\mathsf{T}\boldsymbol{\Sigma}^{-1}\boldsymbol{\mu}_y.$$

In words, the Lda classifier chooses the class for whom the projection of an input vector $\boldsymbol{x}$, onto $\boldsymbol{\Sigma}^{-1}\boldsymbol{\mu}_y$, is maximized. When there are only two classes, this further simplies to

$$g_{2-\text{Lda}}(\boldsymbol{x}) := \mathbb{I}\{\boldsymbol{x}^\mathsf{T}\boldsymbol{\Sigma}^{-1}\boldsymbol{\delta} > 0\},$$

where $\boldsymbol{\delta} = \boldsymbol{\mu}_0 - \boldsymbol{\mu}_1$. Note that the equal class prior and centered means assumptions merely changes the threshold constant from 0 to something else.

II.C Lda Model

A statistical model is a family of distributions indexed by a parameter $\boldsymbol{\theta} \in \Theta$, $\mathcal{F}_{\boldsymbol{\theta}} = \{F_{\boldsymbol{\theta}} : \boldsymbol{\theta} \in \Theta\}$. Consider the special case of the above where $F_{\boldsymbol{X}|Y=y}$ is a multivariate Gaussian distribution, $\mathcal{N}(\boldsymbol{\mu}_y, \boldsymbol{\Sigma})$, where each class has its own mean, but all classes have the same covariance. We refer to this model as the Lda model. Let $\boldsymbol{\theta} = (\boldsymbol{\pi}, \boldsymbol{\mu}, \boldsymbol{\Sigma})$, and let $\Theta_{C-\text{Lda}} = (\triangle_C, \mathbb{R}^{p \times C}, \mathbb{R}_{\succ 0}^{p \times p})$, where $\boldsymbol{\mu} = (\boldsymbol{\mu}_1, \ldots, \boldsymbol{\mu}_C)$, $\triangle_C$ is the C dimensional simplex, that is $\triangle_C = \{\boldsymbol{x} : x_i \geq 0 \forall i, \sum_i x_i = 1\}$, and $\mathbb{R}_{\succ 0}^{p \times p}$ is the set of positive definite $p \times p$ matrices. Denote $\mathcal{F}_{\text{Lda}} = \{F_{\boldsymbol{\theta}} : \boldsymbol{\theta} \in \Theta_{\text{Lda}}\}$, dropping the superscript C for brevity where appropriate. The following lemma is well known:

Lemma 1. $L^F_{Lda} = L^F_*$ *for any* $F \in \mathcal{F}_{Lda}$.

Proof. Under the LDA model, the Bayes optimal classifier is available by plugging the explicit distributions into Eq. (1). $\qquad\square$

C   Projection Based Classifiers

Let $A \in \mathbb{R}^{d \times p}$ be an orthonormal matrix, that is, a matrix that projects p dimensional data into a d dimensional subspace, where AA^T is the $d \times d$ identity matrix, and $A^\mathsf{T}A$ skis symmetric $p \times p$ matrix with rank d. The question that motivated this work is: what is the best projection matrix that we can estimate, to use to "pre-process" the data prior to applying LDA. Projecting the data x onto a low-dimensional subspace, and the classifying via LDA in that subspace is equivalent to redefining the parameters in the low-dimensional subspace, $\Sigma_A = A\Sigma A^\mathsf{T} \in \mathbb{R}^{d \times d}$ and $\delta_A = A\delta \in \mathbb{R}^d$, and then using g_{Lda}. When $C = 2$, $\pi_0 = \pi_1$, and $(\mu_0 + \mu_1)/2 = \mathbf{0}$, this amounts to:

$$g^d_A(x) := \mathbb{I}\{(Ax)^\mathsf{T}\Sigma^{-1}_A\delta_A > 0\}, \text{ where } A \in \mathbb{R}^{d \times p}. \tag{2}$$

Let $L^d_A := \int \mathbb{P}[g_A(x) = y]f_{x,y}dxdy$. Our goal therefore is to be able to choose A for a given parameter setting $\theta = (\pi, \delta, \Sigma)$, such that L_A is as small as possible (note that L_A will never be smaller than L_*).

Formally, we seek to solve the following optimization problem:

$$\begin{aligned} \underset{A}{\text{minimize}} \quad & \mathbb{E}[\mathbb{I}\{x^\mathsf{T}A^\mathsf{T}\Sigma^{-1}_A\delta_A > 0\} \neq y] \\ \text{subject to} \quad & A \in \mathbb{R}^{p \times d}, \quad AA^\mathsf{T} = I_{d \times d}, \end{aligned} \tag{3}$$

where $I_{u \times v}$ is the $u \times v$ identity matrix identity, that is, $I(i,j) = 1$ for all $i = j \leq \min(u,v)$, and zero otherwise. Let $\mathcal{A}^d = \{A : A \in \mathbb{R}^{d \times p}, AA^\mathsf{T} = I_{d \times d}\}$, and let $\mathcal{A}_* \subset \mathcal{A}$ be the set of A that minimize Eq. (3), and let $A_* \in \mathcal{A}_*$ (where we dropped the superscript d for brevity). Let $L^*_A = L_{A_*}$ be the misclassification rate for any $A \in \mathcal{A}_*$, that is, L^*_A is the Bayes optimal misclassification rate for the classifier that composes A with LDA.

In our opinion, Eq. (3) is the simplest supervised manifold learning problem there is: a two-class classification problem, where the data are multivariate Gaussians with shared covariances, the manifold is linear, and the classification is done via LDA. Nonetheless, solving Eq. (3) is difficult, because we do not know how to evaluate the integral analytically, and we do not know any algorithms that are guaranteed to find the global optimum in finite time. This has led to previous work using a surrogate function [**?**]. We proceed by studying a few natural choices for A.

III.A   Bayes Optimal Projection

Lemma 2. $\delta^\mathsf{T}\Sigma^{-1} \in \mathcal{A}_*$

Proof. Let $B = (\Sigma^{-1}\delta)^\mathsf{T} = \delta^\mathsf{T}(\Sigma^{-1})^\mathsf{T} = \delta^\mathsf{T}\Sigma^{-1}$, so that $B^\mathsf{T} = \Sigma^{-1}\delta$, and plugging this in to Eq. (2), we obtain

$$\begin{aligned} g_B(x) &= \mathbb{I}\{xB^\mathsf{T}\Sigma^{-1}_B\delta_B > 0\} \\ &= \mathbb{I}\{x^\mathsf{T}\Sigma^{-1}\delta \times (\Sigma^{-1}_B\delta_B) > 0\} && \text{plugging in } B \\ &= \mathbb{I}\{x^\mathsf{T}\Sigma^{-1}\delta k > 0\} && \text{because } \Sigma^{-1}_B\delta_B > 0. \end{aligned}$$

In other words, letting B be the Bayes optimal projection recovers the Bayes classifier, as it should. Or, more formally, for any $F \in \mathcal{F}_{\mathrm{Lda}}$, $L_{\delta^\mathsf{T}\Sigma^{-1}} = L_*$ $\qquad\square$

III.B   **Principle Components Analysis (**PCA**) Projection**

436   Principle Components Analysis (PCA) finds the directions of maximal variance in a dataset. PCA is closely
437   related to eigendecompositions and singular value decompositions (SVD). In particular, the top principle
438   component of a matrix $\boldsymbol{X} \in \mathbb{R}^{p \times n}$, whose columns are centered, is the eigenvector with the largest corre-
439   sponding eigenvalue of the centered covariance matrix $\boldsymbol{X}\boldsymbol{X}^{\top}$. SVD enables one to estimate this eigenvector
440   without ever forming the outer product matrix, because SVD factorizes a matrix $\boldsymbol{X}$ into $\boldsymbol{U}\boldsymbol{S}\boldsymbol{V}^{\top}$, where $\boldsymbol{U}$
441   and $\boldsymbol{V}$ are orthonormal $p \times n$ matrices, and $\boldsymbol{S}$ is a diagonal matrix, whose diagonal values are decreasing,
442   $s_1 \geq s_2 \geq \cdots > s_n$. Defining $\boldsymbol{U} = [\boldsymbol{u}_1, \boldsymbol{u}_2, \ldots, \boldsymbol{u}_n]$, where each $\boldsymbol{u}_i \in \mathbb{R}^p$, then $\boldsymbol{u}_i$ is the ith eigenvector, and s_i
443   is the square root of the ith eigenvalue of $\boldsymbol{X}\boldsymbol{X}^{\top}$. Let $\boldsymbol{A}_d^{\texttt{Pca}} = [\boldsymbol{u}_1, \ldots, \boldsymbol{u}_d]$ be the truncated PCA orthonormal
444   matrix.

The PCA matrix is perhaps the most obvious choice of a orthonormal matrix for several reasons. First,
truncated PCA minimizes the squared error loss between the original data matrix and all possible rank d
representations:

$$\operatorname*{argmin}_{A \in \mathbb{R}^{d \times p} : \boldsymbol{A}\boldsymbol{A}^{\top} = \boldsymbol{I}_{d \times d}} \left\| \boldsymbol{X} - \boldsymbol{A}^T \boldsymbol{A} \right\|_F^2 .$$

446   Second, the ubiquity of PCA has led to a large number of highly optimized numerical libraries for computing
447   PCA (for example, LAPACK [33]).

448   Moreover, let $\boldsymbol{U}_d = [\boldsymbol{u}_1, \ldots, \boldsymbol{u}_d] \in \mathbb{R}^{p \times d}$, and note that $\boldsymbol{U}_d^{\top}\boldsymbol{U}_d = \boldsymbol{I}_{d \times p}$ and $\boldsymbol{U}_d^{\top}\boldsymbol{U}_d = \boldsymbol{I}_{p \times d}$. Similarly, let
449   $\boldsymbol{U}\boldsymbol{S}\boldsymbol{U}^{\top} = \boldsymbol{\Sigma}$, and $\boldsymbol{U}\boldsymbol{S}^{-1}\boldsymbol{U}^{\top} = \boldsymbol{\Sigma}^{-1}$. Let $\boldsymbol{S}_d$ be the matrix whose diagonal entries are the eigenvalues, up to
450   the dth one, that is $\boldsymbol{S}_d(i,j) = s_i$ for $i = j \leq d$ and zero otherwise. Similarly, $\boldsymbol{\Sigma}_d = \boldsymbol{U}\boldsymbol{S}_d\boldsymbol{U}^{\top} = \boldsymbol{U}_d\boldsymbol{S}_d\boldsymbol{U}_d^{\top}$.

451   Let $g_{\texttt{Pca}}^d := g_{A_{\texttt{Pca}}^d}$, and let $L_{\texttt{Pca}}^d := L_{A_{\texttt{Pca}}^d}$. And let $g_{\texttt{Lda}}^d := \mathbb{I}\{x\boldsymbol{\Sigma}_d^{-1}\boldsymbol{\delta} > 0\}$ be the regularized LDA classifier, that
452   is, the LDA classifier, but sets the bottom $p - d$ eigenvalues to zero.

453   **Lemma 3.** $L_{Pca}^d = L_{RR-Lda}^d$.

Proof. Plugging $\boldsymbol{U}_d$ into Eq. (2) for $\boldsymbol{A}$, and considering only the left side of the operand, we have

$$
\begin{aligned}
(\boldsymbol{A}\boldsymbol{x})^{\top}\boldsymbol{\Sigma}_A^{-1}\boldsymbol{\delta}_A &= \boldsymbol{x}^{\top}\boldsymbol{A}^{\top}\boldsymbol{A}\boldsymbol{\Sigma}^{-1}\boldsymbol{A}^{\top}\boldsymbol{A}\boldsymbol{\delta}, \\
&= \boldsymbol{x}^{\top}\boldsymbol{U}_d\boldsymbol{U}_d^{\top}\boldsymbol{\Sigma}^{-1}\boldsymbol{U}_d\boldsymbol{U}_d^{\top}\boldsymbol{\delta}, \\
&= \boldsymbol{x}^{\top}\boldsymbol{U}_d\boldsymbol{U}_d^{\top}\boldsymbol{U}\boldsymbol{S}^{-1}\boldsymbol{U}\boldsymbol{U}_d\boldsymbol{U}_d^{\top}\boldsymbol{\delta}, \\
&= \boldsymbol{x}^{\top}\boldsymbol{U}_d\boldsymbol{I}_{d \times p}\boldsymbol{S}^{-1}\boldsymbol{I}_{p \times d}\boldsymbol{U}_d^{\top}\boldsymbol{\delta}, \\
&= \boldsymbol{x}^{\top}\boldsymbol{U}_d\boldsymbol{S}_d^{-1}\boldsymbol{U}_d^{\top}\boldsymbol{\delta}, \\
&= \boldsymbol{x}^{\top}\boldsymbol{\Sigma}_d^{-1}\boldsymbol{\delta}.
\end{aligned}
$$

454   □

455   The implication of this lemma is that if one desires to implement RR-LDA, rather than first learning the
456   eigenvectors and then learning LDA, one can instead directly implement regularized LDA by setting the
457   bottom $p - d$ eigenvalues to zero.

III.C   **Linear Optimal Low-Rank (**LOL**) Projection**

459   The basic idea of LOL is to use both $\boldsymbol{\delta}$ and the top d eigenvectors. Most naïvely, we could simply concatenate
460   the two, $\boldsymbol{A}_{\texttt{Lol}}^d = [\boldsymbol{\delta}, \boldsymbol{A}_{\texttt{Pca}}^{d-1}]$. Recall that eigenvectors are orthonormal. To maintain orthonormality, we could
461   easily apply Gram-Schmidt, $\boldsymbol{A}_{\texttt{Lol}}^d = \texttt{ORTH}([\boldsymbol{\delta}, \boldsymbol{A}_{\texttt{Pca}}^{d-1}])$. Both in practice and in theory (as will be shown
462   below), this orthogonalization step does not matter much.

463   to ensure that they are balanced appropriately, we normalize $\boldsymbol{\delta}$

464   each vector in $\boldsymbol{\delta}$ to have norm unity. Formally, let $\widetilde{\boldsymbol{\delta}}_j = \boldsymbol{\delta}_j / \|\boldsymbol{\delta}_j\|$, where $\boldsymbol{\delta}_j$ is the jth difference of the
465   mean vector (remember, the number of vectors is equal to $C - 1$, where C is the total number of classes),

⁴⁶⁶ and let $\boldsymbol{A}_{\mathtt{Lol}}^d = [\widetilde{\boldsymbol{\delta}}, \boldsymbol{A}_{\mathtt{Pca}}^{d-(C-1)}]$. The eigenvectors are all normalized and orthogonal to one another; to
⁴⁶⁷ impose orthogonality between $\widetilde{\delta}$ and the eigenvectors, we could use any number of numerically optimized
⁴⁶⁸ algorithms. However, in practice, orthogonalizing does not matter very much, so we do not bother. We
⁴⁶⁹ formally demonstrate this below.

⁴⁷⁰ D   Theoretical Properties of LDA based Classifiers

⁴⁷¹ IV.A $\mathtt{LDA}$ is rotationally invariant

⁴⁷² For certain classification tasks, the ambient coordinates have intrinsic value, for example, when simple
⁴⁷³ interpretability is desired. However, in many other contexts, interpretability is less important [**?**]. When
⁴⁷⁴ the exploitation task at hand is invariant to rotations, then we have no reason to restrict our search space
⁴⁷⁵ to be sparse in the ambient coordinates, rather, for example, we can consider sparsity in the eigenvector
⁴⁷⁶ basis. Fisherfaces is one example of a rotationally invariant classifier, under certain model assumptions.
⁴⁷⁷ Let $\boldsymbol{W}$ be a rotation matrix, that is $\boldsymbol{W} \in \mathcal{W} = \{\boldsymbol{W} : \boldsymbol{W}^\mathsf{T} = \boldsymbol{W}^{-1}$ and $\det(\boldsymbol{W}) = 1\}$. Moreover, let
⁴⁷⁸ $\boldsymbol{W} \circ F$ denote the distribution F after transformation by an operator $\boldsymbol{W}$. For example, if $F = \mathcal{N}(\boldsymbol{\mu}, \boldsymbol{\Sigma})$ then
⁴⁷⁹ $\boldsymbol{W} \circ F = \mathcal{N}(\boldsymbol{W}\boldsymbol{\mu}, \boldsymbol{W}\boldsymbol{\Sigma}\boldsymbol{W}^\mathsf{T})$.

Definition 1. *A rotationally invariant classifier has the following property:*

$$L_g^F = L_g^{W \circ F}, \qquad F \in \mathcal{F}.$$

⁴⁸⁰ *In words, the Bayes risk of using classifier g on distribution F is unchanged if F is first rotated, for any*
⁴⁸¹ $F \in \mathcal{F}$.

⁴⁸² Now, we can state the main lemma of this subsection: $\mathtt{LDA}$ is rotationally invariant.

⁴⁸³ **Lemma 4.** $L_{Lda}^F = L_{Lda}^{W \circ F}$, *for any $F \in \mathcal{F}$.*

⁴⁸⁴ *Proof.* $\mathtt{LDA}$ simply becomes thresholding $\boldsymbol{x}^\mathsf{T}\boldsymbol{\Sigma}^{-1}\boldsymbol{\delta}$. Thus, we can demonstrate rotational invariance by
⁴⁸⁵ demonstrating that $\boldsymbol{x}^\mathsf{T}\boldsymbol{\Sigma}^{-1}\boldsymbol{\delta}$ is rotationally invariant.

$$
\begin{aligned}
(\boldsymbol{W}\boldsymbol{x})^\mathsf{T}(\boldsymbol{W}\boldsymbol{\Sigma}\boldsymbol{W}^\mathsf{T})^{-1}\boldsymbol{W}\boldsymbol{\delta} &= \boldsymbol{x}^\mathsf{T}\boldsymbol{W}^\mathsf{T}(\boldsymbol{W}\boldsymbol{U}\boldsymbol{S}\boldsymbol{U}^\mathsf{T}\boldsymbol{W}^\mathsf{T})^{-1}\boldsymbol{W}\boldsymbol{\delta} && \text{by substituting } \boldsymbol{U}\boldsymbol{S}\boldsymbol{U}^\mathsf{T} \text{ for } \boldsymbol{\Sigma} \\
&= \boldsymbol{x}^\mathsf{T}\boldsymbol{W}^\mathsf{T}(\widetilde{\boldsymbol{U}}\boldsymbol{S}\widetilde{\boldsymbol{U}}^\mathsf{T})^{-1}\boldsymbol{W}\boldsymbol{\delta} && \text{by letting } \widetilde{\boldsymbol{U}} = \boldsymbol{W}\boldsymbol{U} \\
&= \boldsymbol{x}^\mathsf{T}\boldsymbol{W}^\mathsf{T}(\widetilde{\boldsymbol{U}}\boldsymbol{S}^{-1}\widetilde{\boldsymbol{U}}^\mathsf{T})\boldsymbol{W}\boldsymbol{\delta} && \text{by the laws of matrix inverse} \\
&= \boldsymbol{x}^\mathsf{T}\boldsymbol{W}^\mathsf{T}\boldsymbol{W}\boldsymbol{U}\boldsymbol{S}^{-1}\boldsymbol{U}^\mathsf{T}\boldsymbol{W}^\mathsf{T}\boldsymbol{W}\boldsymbol{\delta} && \text{by un-substituting } \boldsymbol{W}\boldsymbol{U} = \widetilde{\boldsymbol{U}} \\
&= \boldsymbol{x}^\mathsf{T}\boldsymbol{U}\boldsymbol{S}^{-1}\boldsymbol{U}^\mathsf{T}\boldsymbol{\delta} && \text{because } \boldsymbol{W}^\mathsf{T}\boldsymbol{W} = \boldsymbol{I} \\
&= \boldsymbol{x}^\mathsf{T}\boldsymbol{\Sigma}^{-1}\boldsymbol{\delta} && \text{by un-substituting } \boldsymbol{U}\boldsymbol{S}^{-1}\boldsymbol{U}^\mathsf{T} = \boldsymbol{\Sigma}
\end{aligned}
$$

⁴⁸⁶ $\qquad$ □

⁴⁸⁷ One implication of this lemma is that we can reparameterize without loss of generality. Specifically, defining
⁴⁸⁸ $\boldsymbol{W} := \boldsymbol{U}^\mathsf{T}$ yields a change of variables: $\boldsymbol{\Sigma} \mapsto \boldsymbol{S}$ and $\boldsymbol{\delta} \mapsto \boldsymbol{U}^\mathsf{T}\boldsymbol{\delta} := \boldsymbol{\delta}''$, where $\boldsymbol{S}$ is a diagonal covariance
⁴⁸⁹ matrix. Moreover, let $\boldsymbol{d} = (\sigma_1, \ldots, \sigma_D)^\mathsf{T}$ be the vector of eignevalues, then $\boldsymbol{S}^{-1}\boldsymbol{\delta}' = \boldsymbol{d}^{-1} \odot \widetilde{\boldsymbol{\delta}}$, where
⁴⁹⁰ $\odot$ is the Hadamard (entrywise) product. The $\mathtt{LDA}$ classifier may therefore be encoded by a unit vector,
⁴⁹¹ $\widetilde{\boldsymbol{d}} := \frac{1}{m}\boldsymbol{d}^{-1} \odot \boldsymbol{\delta}'$, and its magnitude, $m := \left\|\boldsymbol{d}^{-1} \odot \widetilde{\boldsymbol{\delta}}\right\|$. This will be useful later.

⁴⁹² IV.B   Rotation of Projection Based Linear Classifiers g_A

⁴⁹³ By a similar argument as above, one can easily show that:

$$(\boldsymbol{A}\boldsymbol{W}\boldsymbol{x})^{\mathsf{T}}(\boldsymbol{A}\boldsymbol{W}\boldsymbol{\Sigma}\boldsymbol{W}^{\mathsf{T}}\boldsymbol{A}^{\mathsf{T}})^{-1}\boldsymbol{A}\boldsymbol{W}\boldsymbol{\delta} = \boldsymbol{x}^{\mathsf{T}}(\boldsymbol{W}^{\mathsf{T}}\boldsymbol{A}^{\mathsf{T}})(\boldsymbol{A}\boldsymbol{W})\boldsymbol{\Sigma}^{-1}(\boldsymbol{W}^{\mathsf{T}}\boldsymbol{A}^{\mathsf{T}})(\boldsymbol{A}\boldsymbol{W})\boldsymbol{\delta}$$
$$= \boldsymbol{x}^{\mathsf{T}}\boldsymbol{Y}^{\mathsf{T}}\boldsymbol{Y}\boldsymbol{\Sigma}^{-1}\boldsymbol{Y}^{\mathsf{T}}\boldsymbol{Y}\boldsymbol{\delta}$$
$$= \boldsymbol{x}^{\mathsf{T}}\boldsymbol{Z}\boldsymbol{\Sigma}^{-1}\boldsymbol{Z}^{\mathsf{T}}\boldsymbol{\delta}$$
$$= \boldsymbol{x}^{\mathsf{T}}(\boldsymbol{Z}\boldsymbol{\Sigma}\boldsymbol{Z}^{\mathsf{T}})^{-1}\boldsymbol{\delta} = \boldsymbol{x}^{\mathsf{T}}\widetilde{\boldsymbol{\Sigma}}_d^{-1}\boldsymbol{\delta},$$

where $\boldsymbol{Y} = \boldsymbol{A}\boldsymbol{W} \in \mathbb{R}^{d \times p}$ so that $\boldsymbol{Z} = \boldsymbol{Y}^{\mathsf{T}}\boldsymbol{Y}$ is a symmetric $p \times p$ matrix of rank d. In other words, rotating and then projecting is equivalent to a change of basis. The implications of the above is:

Lemma 5. g_A *is rotationally invariant if and only if span($\boldsymbol{A}$)=span($\boldsymbol{\Sigma}_d$). In other words,* PCA *is the only rotationally invariant projection.*

IV.C   Chernoff information

We now introduce the notion of the Chernoff information, which serves as our surrogate measure for the Bayes error of any classification procedure given the *projected* data – in the context of this paper the projection is via LoL or PCA. Our discussion of the Chernoff information is under the context of decision rules for hypothesis testing, nevertheless, as evidenced by the fact that the Maximum A Posterior decision rule – equivalently the Bayes classifier – achieves the Chernoff information rate, this distinction between hypothesis testing and classification is mainly for ease of exposition.

Let F_0 and F_1 be two absolutely continuous multivariate distribution in $\Omega \subset \mathbb{R}^d$ with density function f_0 and f_1, respectively. Suppose that $Y_1, Y_2, \ldots, Y_m$ are independent and identically distributed random variables, with Y_i distributed either F_0 or F_1. We are interested in testing the simple null hypothesis $\mathbb{H}_0 \colon F = F_0$ against the simple alternative hypothesis $\mathbb{H}_1 \colon F = F_1$. A test T is a sequence of mapping $T_m \colon \Omega^m \mapsto \{0, 1\}$ such that given $Y_1 = y_1, Y_2 = y_2, \ldots, Y_m = y_m$, the test rejects $\mathbb{H}_0$ in favor of $\mathbb{H}_1$ if $T_m(y_1, y_2, \ldots, y_m) = 1$; similarly, the test rejects $\mathbb{H}_1$ in favor of $\mathbb{H}_0$ if $T_m(y_1, y_2, \ldots, y_m) = 0$. The Neyman-Pearson lemma states that, given $Y_1 = y_1, Y_2 = y_2, \ldots, Y_m = y_m$ and a threshold $\eta_m \in \mathbb{R}$, the likelihood ratio test which rejects $\mathbb{H}_0$ in favor of $\mathbb{H}_1$ whenever

$$\left(\sum_{i=1}^m \log f_0(y_i) - \sum_{i=1}^m \log f_1(y_i) \right) \leq \eta_m$$

is the most powerful test at significance level $\alpha_m = \alpha(\eta_m)$, i.e., the likelihood ratio test minimizes the type-II error β_m subject to the contraint that the type-I error is at most α_m.

Assuming that $\pi \in (0, 1)$ is a prior probability that $\mathbb{H}_0$ is true. Then, for a given $\alpha_m^* \in (0, 1)$, let $\beta_m^* = \beta_m^*(\alpha_m^*)$ be the type-II error associated with the likelihood ratio test when the type-I error is at most α_m^*. The quantity $\inf_{\alpha_m^* \in (0,1)} \pi\alpha_m^* + (1-\pi)\beta_m^*$ is then the Bayes risk in deciding between $\mathbb{H}_0$ and $\mathbb{H}_1$ given the m independent random variables $Y_1, Y_2, \ldots, Y_m$. A classical result of Chernoff [34] states that the Bayes risk is intrinsically linked to a quantity known as the *Chernoff information*. More specifically, let $C(F_0, F_1)$ be the quantity

$$C(F_0, F_1) = -\log \left[\inf_{t \in (0,1)} \int_{\mathbb{R}^d} f_0^t(\boldsymbol{x}) f_1^{1-t}(\boldsymbol{x}) \mathrm{d}\boldsymbol{x} \right]$$
$$= \sup_{t \in (0,1)} \left[-\log \int_{\mathbb{R}^d} f_0^t(\boldsymbol{x}) f_1^{1-t}(\boldsymbol{x}) \mathrm{d}\boldsymbol{x} \right] \tag{4}$$

Then we have

$$\lim_{m \to \infty} \frac{1}{m} \inf_{\alpha_m^* \in (0,1)} \log(\pi\alpha_m^* + (1-\pi)\beta_m^*) = -C(F_0, F_1). \tag{5}$$

Thus $C(F_0, F_1)$ is the *exponential* rate at which the Bayes error $\inf_{\alpha_m^* \in (0,1)} \pi\alpha_m^* + (1-\pi)\beta_m^*$ decreases as $m \to \infty$; we also note that the $C(F_0, F_1)$ is independent of π. We also define, for a given $t \in (0, 1)$ the Chernoff divergence $C_t(F_0, F_1)$ between F_0 and F_1 by

$$C_t(F_0, F_1) = -\log \int_{\mathbb{R}^d} f_0^t(\boldsymbol{x}) f_1^{1-t}(\boldsymbol{x}) \mathrm{d}\boldsymbol{x}.$$

D. LDA

513   The Chernoff divergence is an example of a f-divergence as defined in [35]. When $t = 1/2$, $C_t(F_0, F_1)$ is
514   the Bhattacharyya distance between F_0 and F_1.

515   The result of Eq. (5) can be extended to $K + 1 \geq 2$ hypothesis, with the exponential rate being the min-
516   imum of the Chernoff information between any pair of hypothesis. More specifically, let $F_0, F_1, \ldots, F_K$ be
517   distributions on $\mathbb{R}^d$ and let $Y_1, Y_2, \ldots, Y_m$ be independent and identically distributed random variables with
518   distribution $F \in \{F_0, F_1, \ldots, F_K\}$. Our inference task is in determining the distribution of the Y_i among the
519   $K + 1$ hypothesis $\mathbb{H}_0 \colon F = F_0, \ldots, \mathbb{H}_K \colon F = F_K$. Suppose also that hypothesis $\mathbb{H}_k$ has *a priori* probability
520   π_k. For any decision rule δ, the risk of δ is $r(\delta) = \sum_k \pi_k \sum_{l \neq k} \alpha_{lk}(\delta)$ where $\alpha_{lk}(\delta)$ is the probability of
521   accepting hypothesis $\mathbb{H}_l$ when hypothesis $\mathbb{H}_k$ is true. Then we have [36]

$$\inf_{\delta} \lim_{m \to \infty} \frac{r(\delta)}{m} = -\min_{k \neq l} C(F_k, F_l). \tag{6}$$

522   where the infimum is over all decision rule δ, i.e., for any δ, $r(\delta)$ decreases to 0 as $m \to \infty$ at a rate no
523   faster than $\exp(-m \min_{k \neq l} C(F_k, F_l))$.

When the distributions F_0 and F_1 are multivariate normal, that is, $F_0 = \mathcal{N}(\mu_0, \Sigma_0)$ and $F_1 = \mathcal{N}(\mu_1, \Sigma_1)$; then,
denoting by $\Sigma_t = t\Sigma_0 + (1-t)\Sigma_1$, we have

$$C(F_0, F_1) = \sup_{t \in (0,1)} \left(\frac{t(1-t)}{2} (\mu_1 - \mu_2)^\top \Sigma_t^{-1} (\mu_1 - \mu_2) + \frac{1}{2} \log \frac{|\Sigma_t|}{|\Sigma_0|^t |\Sigma_1|^{1-t}} \right).$$

524   IV.D   Projecting data and Chernoff information

525   We now discuss how the Chernoff information characterizes the effect a linear transformation A of the data
526   has on classification accuracy. We start with the following simple result whose proof follows directly from
527   Eq. (6).

528   **Lemma 6.** *Let $F_0 = \mathcal{N}(\mu_0, \Sigma)$ and $F_1 \sim \mathcal{N}(\mu_1, \Sigma)$ be two multivariate normals with equal covariance*
529   *matrices. For any linear transformation A, let $F_0^{(A)}$ and $F_1^{(A)}$ denotes the distribution of AX when $X \sim F_0$*
530   *and $X \sim F_1$, respectively. We then have*

$$\begin{aligned}
C(F_0^{(A)}, F_1^{(A)}) &= \frac{1}{8} (\mu_1 - \mu_0)^\top A^\top (A \Sigma A^\top)^{-1} A (\mu_1 - \mu_0) \\
&= \frac{1}{8} (\mu_1 - \mu_0)^\top \Sigma^{-1/2} \Sigma^{1/2} A^\top (A \Sigma A^\top)^{-1} A \Sigma^{1/2} \Sigma^{-1/2} (\mu_1 - \mu_0) \\
&= \frac{1}{8} \| P_{\Sigma^{1/2} A^\top} \Sigma^{-1/2} (\mu_1 - \mu_0) \|_F^2
\end{aligned} \tag{7}$$

531   *where $P_Z = Z(Z^\top Z)^{-1} Z^\top$ denotes the matrix corresponding to the orthogonal projection onto the columns*
532   *of Z.*

Thus for a classification problem where $X|Y = 0$ and $X|Y = 1$ are distributed multivariate normals with
mean μ_0 and μ_1 and the same covariance matrix Σ, Lemma 6 then states that for any two linear transfor-
mations A and B, the transformed data AX is to be preferred over the transformed data BX if

$$(\mu_1 - \mu_0)^\top A^\top (A \Sigma A^\top)^{-1} A (\mu_1 - \mu_0) > (\mu_1 - \mu_0)^\top B^\top (B \Sigma B^\top)^{-1} B (\mu_1 - \mu_0).$$

As an example, suppose Σ is diagonal with distinct eigenvalues where the diagonal entries of Σ are in
non-increasing order. Denote by $\delta = \mu_1 - \mu_0$ and let $A = \delta^\top$ and $B = e_1^\top = (1, 0, 0, \ldots, 0)$ be the linear
transformations for $\textsc{Lol}$ and PCA of X into $\mathbb{R}$. We then have

$$C(F_0^{(A)}, F_1^{(A)}) = \frac{(\delta^\top \delta)^2}{\delta^\top \Sigma \delta} = \frac{(\sum_i \delta_i^2)^2}{\sum_i \delta_i^2 \lambda_i}; \quad C(F_0^{(B)}, F_1^{(B)}) = \frac{\delta_1^2}{\lambda_1}$$

22

where λ_1 is the largest eigenvalue of Σ. Suppose furthermore that $\delta_1 \leq \delta_2 \leq \cdots \leq \delta_p$ and $\lambda_1 > \lambda_2 > \cdots > \lambda_p$. Then $C(F_0^{(A)}, F_1^{(A)})$ can be lower-bounded as

$$C(F_0^{(A)}, F_1^{(A)}) = \frac{(\sum_i \delta_i^2)^2}{\sum_i \delta_i^2 \lambda_i} \geq \frac{(p\delta_1^2)^2}{p\delta_p^2 \lambda_1}$$

533 and hence $C(F_0^{(A)}, F_1^{(A)}) > C(F_0^{(B)}, F_1^{(B)})$ provided $p\delta_1^2 \geq \delta_p^2$.

When $A = \begin{bmatrix} \delta \mid e_1 \mid e_2 \cdots \mid e_{d-1} \end{bmatrix}^\top \in \mathbb{R}^{d \times p}$ and $B = \begin{bmatrix} e_1 \mid e_2 \mid \cdots \mid e_d \end{bmatrix}^\top \in \mathbb{R}^{d \times p}$ are the linear transformation for LoL and PCA of X into $\mathbb{R}^d$, we have

$$C(F_0^{(A)}, F_1^{(A)}) = \frac{(\sum_{i=d}^p \delta_i^2)^2}{\sum_{i=d}^p \delta_i^2 \lambda_i} + \sum_{i=1}^{d-1} \frac{\delta_i^2}{\lambda_i}; \quad C(F_0^{(B)}, F_1^{(B)}) = \sum_{i=1}^d \frac{\delta_i^2}{\lambda_i}.$$

534 This can be seen as follows. Let $\xi_{d-1} = \begin{bmatrix} e_1 \mid e_2 \mid \cdots \mid e_{d-1} \end{bmatrix} \in \mathbb{R}^{p \times (d-1)}$ and $\zeta_{d-1} = (\lambda_1 \delta_1, \lambda_2 \delta_2, \ldots, \lambda_{d-1}\delta_{d-1})^\top \in$
535 $\mathbb{R}^{d-1}$. Then

$$A\Sigma A^\top = \begin{bmatrix} \delta \mid \xi_{d-1} \end{bmatrix}^\top \Sigma \begin{bmatrix} \delta \mid \xi_{d-1} \end{bmatrix} = \begin{bmatrix} \delta^\top \Sigma \delta & \delta^\top \Sigma \xi_{d-1} \\ \xi_{d-1}^\top \Sigma \delta & \xi_{d-1}^\top \Sigma \xi_{d-1} \end{bmatrix} = \begin{bmatrix} \sum_{i=1}^p \delta_i^2 \lambda_i & \zeta_{d-1}^\top \\ \zeta_{d-1} & \Sigma_{d-1} \end{bmatrix} \tag{8}$$

536 where $\Sigma_{d-1} = \mathrm{diag}(\lambda_1, \lambda_2, \ldots, \lambda_{d-1})$ is the submatrix of Σ corresponding to the eigenvalues $\lambda_1, \lambda_2, \ldots, \lambda_{d-1}$.
537 Using a formula for the inverse of a partitioned matrix, we have

$$(A\Sigma A^\top)^{-1} = \begin{bmatrix} \sum_{i=1}^p \delta_i^2 \lambda_i & \zeta_{d-1}^\top \\ \zeta_{d-1} & \Sigma_{d-1} \end{bmatrix}^{-1}$$
$$= \begin{bmatrix} \left(\sum_{i=1}^p \delta_i^2 \lambda_i - \zeta_{d-1}^\top \Sigma_{d-1}^{-1} \zeta_{d-1}\right)^{-1} & -\left(\sum_i \delta_i^2 \lambda_i - \zeta_{d-1}^\top \Sigma_{d-1}^{-1} \zeta_{d-1}\right)^{-1} \zeta_{d-1}^\top \Sigma_{d-1}^{-1} \\ -\Sigma_{d-1}^{-1} \zeta_{d-1}\left(\sum_i \delta_i^2 \lambda_i - \zeta_{d-1}^\top \Sigma_{d-1}^{-1} \zeta_{d-1}\right)^{-1} & \Sigma_{d-1}^{-1} + \Sigma_{d-1}^{-1} \zeta_{d-1}\left(\sum_i \delta_i^2 \lambda_i - \zeta_{d-1}^\top \Sigma_{d-1}^{-1} \zeta_{d-1}\right)^{-1} \zeta_{d-1}^\top \Sigma_{d-1}^{-1} \end{bmatrix} \tag{9}$$

538 Now, $\sum_{i=1}^p \delta_i^2 \lambda_i - \zeta_{d-1}^\top \Sigma_{d-1}^{-1} \zeta_{d-1} = \sum_{i=1}^p \delta_i^2 - \sum_{i=1}^{d-1} \delta_i^2 \lambda_i = \sum_{i=d}^p \delta_i^2 \lambda_i$. Therefore,

$$(A\Sigma A^\top)^{-1} = \begin{bmatrix} \left(\sum_{i=d}^p \delta_i^2 \lambda_i\right)^{-1} & -\frac{\zeta_{d-1}^\top \Sigma_{d-1}^{-1}}{\sum_{i=d}^p \delta_i^2 \lambda_i} \\ -\frac{\Sigma_{d-1}^{-1} \zeta_{d-1}}{\sum_{i=d}^p \delta_i^2 \lambda_i} & \Sigma_{d-1}^{-1} + \frac{\Sigma_{d-1}^{-1} \zeta_{d-1} \zeta_{d-1}^\top \Sigma_{d-1}^{-1}}{\sum_{i=d}^p \delta_i^2 \lambda_i} \end{bmatrix}. \tag{10}$$

In addition, $A(\mu_1 - \mu_0) = (\delta^\top \delta, \delta_1, \delta_2, \ldots, \delta_{d-1})^\top = (\delta^\top \delta, \zeta_{d-1}^\top \Sigma_{d-1}^{-1})^\top \in \mathbb{R}^d$. Hence

$$(\mu_1 - \mu_0)^\top A^\top (A\Sigma A^\top)^{-1} A(\mu_1 - \mu_0) = \begin{bmatrix} \delta^\top \delta \mid \zeta_{d-1}^\top \Sigma_{d-1}^{-1} \end{bmatrix} \begin{bmatrix} \left(\sum_{i=d}^p \delta_i^2 \lambda_i\right)^{-1} & -\frac{\zeta_{d-1}^\top \Sigma_{d-1}^{-1}}{\sum_{i=d}^p \delta_i^2 \lambda_i} \\ -\frac{\Sigma_{d-1}^{-1} \zeta_{d-1}}{\sum_{i=d}^p \delta_i^2 \lambda_i} & \Sigma_{d-1}^{-1} + \frac{\Sigma_{d-1}^{-1} \zeta_{d-1} \zeta_{d-1}^\top \Sigma_{d-1}^{-1}}{\sum_{i=d}^p \delta_i^2 \lambda_i} \end{bmatrix} \begin{bmatrix} \delta^\top \delta \\ \Sigma_{d-1}^{-1} \zeta_{d-1} \end{bmatrix}$$
$$= \frac{(\delta^\top \delta)^2}{\sum_{i=d}^p \delta_i^2 \lambda_i} - 2\delta^\top \delta \frac{\zeta_{d-1}^\top \Sigma_{d-1}^{-2} \zeta_{d-1}}{\sum_{i=d}^p \delta_i^2 \lambda_i} + \left(\zeta_{d-1}^\top \Sigma_{d-1}^{-3} \zeta_{d-1} + \frac{(\zeta_{d-1}^\top \Sigma_{d-1}^{-2} \zeta_{d-1})^2}{\sum_{i=d}^p \delta_i^2 \lambda_i}\right)$$
$$= \frac{(\delta^\top \delta - \zeta_{d-1}^\top \Sigma_{d-1}^{-2} \zeta_{d-1})^2}{\sum_{i=d}^p \delta_i^2 \lambda_i} + \zeta_{d-1}^\top \Sigma_{d-1}^{-3} \zeta_{d-1}$$
$$= \frac{\left(\sum_{i=1}^p \delta_i^2 - \sum_{i=1}^{d-1} \delta_i^2\right)^2}{\sum_{i=d}^p \delta_i^2 \lambda_i} + \sum_{i=1}^{d-1} \frac{\delta_i^2}{\lambda_i} = \frac{\left(\sum_{i=d}^p \delta_i^2\right)^2}{\sum_{i=d}^p \delta_i^2 \lambda_i} + \sum_{i=1}^{d-1} \frac{\delta_i^2}{\lambda_i}.$$

The derivation of $C(F_0^{(B)}, F_1^{(B)})$ is straightforward and will be omitted. We therefore have

$$C(F_0^{(A)}, F_1^{(A)}) - C(F_0^{(B)}, F_1^{(B)}) = \frac{\left(\sum_{i=d}^p \delta_i^2\right)^2}{\sum_{i=d}^p \delta_i^2 \lambda_i} - \frac{\delta_d^2}{\lambda_d}.$$

D. LDA

From our assumption that $\lambda_d \geq \lambda_{d+1} \geq \cdots \geq \lambda_p$, we have $\sum_{i=d}^p \delta_i^2 \lambda_i \leq \lambda_d \sum_{i=d}^p \delta_i^2$ and hence

$$\frac{\left(\sum_{i=d}^p \delta_i^2\right)^2}{\sum_{i=d}^p \delta_i^2 \lambda_i} \geq \frac{\left(\sum_{i=d}^p \delta_i^2\right)^2}{\lambda_d \sum_{i=d}^p \delta_i^2} = \frac{1}{\lambda_d} \sum_{i=d}^p \delta_i^2 \geq \frac{\delta_d^2}{\lambda_d}$$

and hence $C(F_0^{(A)}, F_1^{(A)}) \geq C(F_0^{(B)}, F_1^{(B)})$ always, and the inequality is strict provided that $\sum_{d+1}^p \delta_d^2 > 0$.

Finally we consider the case where Σ is an arbitrary covariance matrix. Let $\lambda_1 \geq \lambda_2 \geq \cdots \geq \lambda_p$ be the eigenvalues of Σ and let $u_1, u_2, \ldots, u_p$ be the corresponding eigenvectors. For $d \leq p$, let $U_{d-1} = \begin{bmatrix} u_1 \mid u_2 \mid \cdots \mid u_{d-1} \end{bmatrix} \in \mathbb{R}^{p \times (d-1)}$ be the matrix whose columns are the eigenvectors $u_1, u_2, \ldots, u_{d-1}$ of Σ. Then the LOL projection matrix into $\mathbb{R}^d$ is given by $A = \begin{bmatrix} \delta | U_{d-1} \end{bmatrix}^\top$. We first have

$$A \Sigma A^\top = \begin{bmatrix} \delta | U_{d-1} \end{bmatrix}^\top \Sigma \begin{bmatrix} \delta | U_{d-1} \end{bmatrix} = \begin{bmatrix} \delta^\top \Sigma \delta & \delta^\top \Sigma U_{d-1} \\ U_{d-1}^\top \Sigma \delta & U_{d-1}^\top \Sigma U_{d-1} \end{bmatrix} = \begin{bmatrix} \delta^\top \Sigma \delta & \delta^\top \Sigma U_{d-1} \\ U_{d-1}^\top \Sigma \delta & \Lambda_{d-1} \end{bmatrix}$$

where $\Lambda_{d-1} = \text{diag}(\lambda_1, \lambda_2, \ldots, \lambda_{d-1})$ is the $(d-1) \times (d-1)$ diagonal matrix formed by the eigenvalues $\lambda_1, \lambda_2, \ldots, \lambda_{d-1}$. Therefore, letting $\gamma = \delta^\top \Sigma \delta - \delta^\top \Sigma U_{d-1} \Lambda_{d-1}^{-1} U_{d-1}^\top \Sigma \delta$, we have

$$(A \Sigma A^\top)^{-1} = \begin{bmatrix} \delta^\top \Sigma \delta & \delta^\top \Sigma U_{d-1} \\ U_{d-1}^\top \Sigma \delta & U_{d-1}^\top \Sigma U_{d-1} \end{bmatrix}^{-1}$$

$$= \begin{bmatrix} \gamma^{-1} & -\delta^\top \Sigma U_{d-1} \Lambda_{d-1}^{-1} \gamma^{-1} \\ -\Lambda_{d-1}^{-1} U_{d-1}^\top \Sigma \delta \gamma^{-1} & \left(\Lambda_{d-1} - \frac{U_{d-1}^\top \Sigma \delta \delta^\top \Sigma U_{d-1}}{\delta^\top \Sigma \delta}\right)^{-1} \end{bmatrix}.$$

The Sherman-Morrison-Woodbury formula then implies

$$\left(\Lambda_{d-1} - \frac{U_{d-1}^\top \Sigma \delta \delta^\top \Sigma U_{d-1}}{\delta^\top \Sigma \delta}\right)^{-1} = \Lambda_{d-1}^{-1} + \frac{\Lambda_{d-1}^{-1} U_{d-1}^\top \Sigma \delta \delta^\top \Sigma U_{d-1} \Lambda_{d-1}^{-1} / (\delta^\top \Sigma \delta)}{1 - \delta^\top \Sigma U_{d-1} \Lambda_{d-1}^{-1} U_{d-1}^\top \Sigma \delta / (\delta^\top \Sigma \delta)}$$

$$= \Lambda_{d-1}^{-1} + \frac{\Lambda_{d-1}^{-1} U_{d-1}^\top \Sigma \delta \delta^\top \Sigma U_{d-1} \Lambda_{d-1}^{-1}}{\delta^\top \Sigma \delta - \delta^\top \Sigma U_{d-1} \Lambda_{d-1}^{-1} U_{d-1}^\top \Sigma \delta}$$

$$= \Lambda_{d-1}^{-1} + \gamma^{-1} \Lambda_{d-1}^{-1} U_{d-1}^\top \Sigma \delta \delta^\top \Sigma U_{d-1} \Lambda_{d-1}^{-1}$$

We note that $\Sigma U_{d-1} = U_{d-1} \Lambda_{d-1}$ and $U_{d-1}^\top \Sigma = \Lambda_{d-1} U_{d-1}^\top$ and hence

$$\gamma = \delta^\top \Sigma \delta - \delta^\top \Sigma U_{d-1} \Lambda_{d-1}^{-1} U_{d-1}^\top \Sigma \delta = \delta^\top \Sigma \delta - \delta^\top U_{d-1} \Lambda_{d-1} \Lambda_{d-1}^{-1} \Lambda_{d-1} U_{d-1}^\top \delta$$

$$= \delta^\top \Sigma \delta - \delta^\top U_{d-1} \Lambda_{d-1} U_{d-1}^\top \delta = \delta^\top (\Sigma - \Sigma_{d-1}) \delta$$

where $\Sigma_{d-1} = U_{d-1} \Lambda_{d-1} U_{d-1}^\top$ is the best rank $d-1$ approximation to Σ with respect to any unitaritly invariant norm. In addition,

$$\Lambda_{d-1}^{-1} U_{d-1}^\top \Sigma \delta \delta^\top \Sigma U_{d-1} \Lambda_{d-1}^{-1} = \Lambda_{d-1}^{-1} \Lambda_{d-1} U_{d-1}^\top \delta \delta^\top U_{d-1} \Lambda_{d-1} \Lambda_{d-1}^{-1} = U_{d-1}^\top \delta \delta^\top U_{d-1}.$$

We thus have

$$(A\Sigma A^\top)^{-1} = \begin{bmatrix} \gamma^{-1} & -\delta^\top \Sigma U_{d-1} \Lambda_{d-1}^{-1} \gamma^{-1} \\ -\Lambda_{d-1}^{-1} U_{d-1}^\top \Sigma \delta \gamma^{-1} & \left(\Lambda_{d-1} - \frac{U_{d-1}^\top \Sigma \delta \delta^\top \Sigma U_{d-1}}{\delta^\top \Sigma \delta}\right)^{-1} \end{bmatrix} = \begin{bmatrix} \gamma^{-1} & -\gamma^{-1} \delta^\top U_{d-1} \\ -\gamma^{-1} U_{d-1}^\top \delta & \Lambda_{d-1}^{-1} + \gamma^{-1} U_{d-1}^\top \delta \delta^\top U_{d-1} \end{bmatrix}.$$

Therefore,

$$\delta^\top A^\top (A\Sigma A^\top)^{-1} A \delta = \delta^\top \begin{bmatrix} \delta \mid U_{d-1} \end{bmatrix} \begin{bmatrix} \gamma^{-1} & -\gamma^{-1} \delta^\top U_{d-1} \\ -\gamma^{-1} U_{d-1}^\top \delta & \Lambda_{d-1}^{-1} + \gamma^{-1} U_{d-1}^\top \delta \delta^\top U_{d-1} \end{bmatrix} \begin{bmatrix} \delta | U_{d-1} \end{bmatrix}^\top \delta$$

$$= \begin{bmatrix} \delta^\top \delta \mid \delta^\top U_{d-1} \end{bmatrix} \begin{bmatrix} \gamma^{-1} & -\gamma^{-1} \delta^\top U_{d-1} \\ -\gamma^{-1} U_{d-1}^\top \delta & \Lambda_{d-1}^{-1} + \gamma^{-1} U_{d-1}^\top \delta \delta^\top U_{d-1} \end{bmatrix} \begin{bmatrix} \delta^\top \delta \\ U_{d-1}^\top \delta \end{bmatrix}$$

$$= \gamma^{-1} (\delta^\top \delta)^2 - 2\gamma^{-1} \delta^\top \delta \delta^\top U_{d-1} U_{d-1}^\top \delta + \delta^\top U_{d-1} (\Lambda_{d-1}^{-1} + \gamma^{-1} U_{d-1}^\top \delta \delta^\top U_{d-1}) U_{d-1}^\top \delta$$

$$= \gamma^{-1} (\delta^\top \delta - \delta^\top U_{d-1} U_{d-1}^\top \delta)^2 + \delta^\top U_{d-1} \Lambda_{d-1}^{-1} U_{d-1}^\top \delta$$

$$= \gamma^{-1} (\delta^\top (I - U_{d-1} U_{d-1}^\top) \delta)^2 + \delta^\top \Sigma_{d-1}^\dagger \delta$$

24

D. LDA

where $\Sigma_{d-1}^{\dagger}$ is the Moore-Penrose pseudo-inverse of Σ_{d-1}. The PCA projection matrix into $\mathbb{R}^d$ is given by $B = U_d^\top$ and hence

$$\delta^\top B^\top (B\Sigma B^\top)^{-1}B\delta = \delta^\top U_d \Lambda_d^{-1} U_d^\top \delta = \delta^\top \Sigma_d^{\dagger}\delta. \tag{11}$$

We thus have

$$
\begin{aligned}
C(F_0^{(A)}, F_1^{(A)}) - C(F_0^{(B)}, F_1^{(B)}) &= \gamma^{-1}(\delta^\top(I - U_{d-1}U_{d-1}^\top)\delta)^2 - \delta^\top(\Sigma_d^{\dagger} - \Sigma_{d-1}^{\dagger})\delta \\
&= \frac{(\delta^\top(I - U_{d-1}U_{d-1}^\top)\delta)^2}{\delta^\top(\Sigma - \Sigma_{d-1})\delta} - \delta^\top(\Sigma_d^{\dagger} - \Sigma_{d-1}^{\dagger})\delta \\
&\geq \frac{(\delta^\top(I - U_{d-1}U_{d-1}^\top)\delta)^2}{\lambda_d \delta^\top(I - U_{d-1}U_{d-1}^\top)\delta} - \frac{1}{\lambda_d}\delta^\top u_d u_d^\top \delta \\
&= \frac{1}{\lambda_d}\delta^\top(I - U_{d-1}U_{d-1})\delta - \frac{1}{\lambda_d}\delta^\top(U_d U_d^\top - U_{d-1}U_{d-1}^\top)\delta \geq 0
\end{aligned}
$$

where we recall that u_d is the d-th column of U_d. Thus $C(F_0^{(A)}, F_1^{(A)}) \geq C(F_0^{(B)}, F_1^{(B)})$ always, and the inequality is strict whenever $\delta^\top(I - U_d U_d^\top)\delta > 0$.

Next we consider the case when $A = \left[\delta | U_{d-1}\right]^\top$ and $B = U_d$ where U_d is an arbitrary $p \times d$ matrix with $U_d^\top U_d = I$, i.e., U_d has d orthonornal columns, and U_{d-1} is the first $d-1$ columns of U_d. A similar derivation to the above yields

$$C(F_0^{(A)}, F_1^{(A)}) = \frac{(\delta^\top \Sigma^{-1/2}(I - V_{d-1}V_{d-1}^\top)\Sigma^{1/2}\delta)^2}{\delta^\top \Sigma^{1/2}(I - V_{d-1}V_{d-1}^\top)\Sigma^{1/2}\delta} + \delta^\top \Sigma^{-1/2}V_{d-1}V_{d-1}^\top \Sigma^{-1/2}\delta \tag{12}$$

$$C(F_0^{(B)}, F_1^{(B)}) = \delta^\top \Sigma^{-1/2}V_d V_d^\top \Sigma^{-1/2}\delta \tag{13}$$

where $V_d V_{d-1}^\top = \Sigma^{1/2}U_d(U_d^\top \Sigma U_d)^{-1}U_d^\top \Sigma^{1/2}$ is the orthogonal projection onto the column space of $\Sigma^{1/2}U_d$. Hence $C(F_0^{(A)}, F_1^{(A)}) > C(F_0^{(B)}, F_1^{(B)})$ if and only if

$$\frac{(\delta^\top \Sigma^{-1/2}(I - V_{d-1}V_{d-1}^\top)\Sigma^{1/2}\delta)^2}{\delta^\top \Sigma^{1/2}(I - V_{d-1}V_{d-1}^\top)\Sigma^{1/2}\delta} > \delta^\top \Sigma^{-1/2}(V_d V_d^\top - V_{d-1}V_{d-1}^\top)\Sigma^{-1/2}\delta.$$

Let $C(F_0^{(A)}, F_1^{(A)})$ and $C(F_0^{(B)}, F_1^{(B)})$ be the Chernoff informations when $A = [\delta \mid U_{d-1}]^\top$ and $B = [\delta \mid U_d]^\top$ where U_{d-1} and U_d contain the eignevectors of the population covariance matrices Σ; similarly, let $\hat{C}(F_0^{(A)}, F_1^{(A)})$ and $\hat{C}(F_0^{(B)}, F_1^{(B)})$ be the Chernoff informations when $A = [\delta \mid \hat{U}_{d-1}]$ and $B = [\delta \mid \hat{U}_d]$ where $\hat{U}_{d-1}$ and $\hat{U}_d$ contain the eigenvectors of the *sample* covariance matrices $\hat{\Sigma}$. Suppose furthermore that $C(F_0^{(A)}, F_1^{(A)}) > C(F_0^{(B)}, F_1^{(B)})$. Then for sufficiently large n, with high probability, $\hat{C}(F_0^{(A)}, F_1^{(A)}) > \hat{C}(F_0^{(B)}, F_1^{(B)})$.

Finally we consider the case when $B = \tilde{U}_d^\top$ where $\tilde{U}_d$ is the $p \times d$ matrix whose columns are the d largest eigenvectors of the *pooled* covariance matrix $\tilde{\Sigma} = \mathbb{E}[(X - \frac{\mu_0 + \mu_1}{2})(X - \frac{\mu_0 + \mu_1}{2})^\top]$. Assume, without loss of generality, that $\mu_1 = -\mu_0 = \mu$. We then have

$$\tilde{\Sigma} = \mathbb{E}[XX^\top] = \pi\Sigma + \pi\mu_0\mu_0^\top + (1-\pi)\Sigma + (1-\pi)\mu_1\mu_1^\top = \Sigma + \mu\mu^\top = \Sigma + \tfrac{1}{4}\delta\delta^\top.$$

Therefore

$$(B\Sigma B^\top)^{-1} = \left(\tilde{U}_d^\top \Sigma \tilde{U}_d\right)^{-1} = \left(\tilde{U}_d^\top(\tilde{\Sigma} - \tfrac{1}{4}\delta\delta^\top)\tilde{U}_d\right)^{-1} = \left(\tilde{S}_d - \tfrac{1}{4}\tilde{U}_d^\top \delta\delta^\top \tilde{U}_d\right)^{-1} = \tilde{S}_d^{-1} + \frac{\tilde{S}_d^{-1}\tilde{U}_d^\top \delta\delta^\top \tilde{U}_d \tilde{S}_d^{-1}}{4 - \delta^\top \tilde{U}_d \tilde{S}_d^{-1}\tilde{U}_d^\top \delta}$$

556 where $\tilde{S}_d$ is the diagonal matrix containing the d largest eigenvalues of $\tilde{\Sigma}$. Hence

$$C(F_0^{(B)}, F_1^{(B)}) = \delta^\top B^\top (B\Sigma B^\top)^{-1} B\delta = \delta^\top \tilde{U}_d \Big(\tilde{S}_d^{-1} + \frac{\tilde{S}_d^{-1}\tilde{U}_d^\top \delta\delta^\top \tilde{U}_d \tilde{S}_d^{-1}}{4 - \delta^\top \tilde{U}_d \tilde{S}_d^{-1}\tilde{U}_d^\top \delta} \Big) \tilde{U}_d^\top \delta$$

$$= \delta^\top \tilde{U}_d \tilde{S}_d^{-1}\tilde{U}_d^\top \delta + \frac{(\delta^\top \tilde{U}_d \tilde{S}_d^{-1}\tilde{U}_d^\top \delta)^2}{4 - \delta^\top \tilde{U}_d \tilde{S}_d^{-1}\tilde{U}_d^\top \delta} \tag{14}$$

$$= \delta^\top \tilde{\Sigma}_d^\dagger \delta + \frac{(\delta^\top \tilde{\Sigma}_d^\dagger \delta)^2}{4 - \delta^\top \tilde{\Sigma}_d^\dagger \delta} = \frac{4\delta^\top \tilde{\Sigma}_d^\dagger \delta}{4 - \delta^\top \tilde{\Sigma}_d^\dagger \delta}.$$

557 where $\tilde{\Sigma}_d = \tilde{U}_d \tilde{S}_d \tilde{U}_d^\top$ is the best rank d approximation to $\tilde{\Sigma} = \Sigma + \frac{1}{4}\delta\delta^\top$.

We recall that the LOL projection $A = [\delta \mid U_{d-1}]^\top$ yields

$$C(F_0^{(A)}, F_1^{(A)}) = \frac{(\delta^\top (I - U_{d-1}U_{d-1}^\top)\delta)^2}{\delta^\top (\Sigma - \Sigma_{d-1})\delta} + \delta^\top \Sigma_{d-1}^\dagger \delta.$$

558 To illustrate the difference between the LOL projection and that based on the eigenvectors of the *pooled*
559 covariance matrix, consider the following simple example. Let $\Sigma = \mathrm{diag}(\lambda_1, \lambda_2, \ldots, \lambda_p)$ be a diagonal matrix
560 with $\lambda_1 \geq \lambda_2 \geq \cdots \geq \lambda_p$. Also let $\delta = (0, 0, \ldots, 0, s)$. Suppose furthermore that $\lambda_p + s^2/4 < \lambda_d$. Then we
561 have $\tilde{\Sigma}_d = \mathrm{diag}(\lambda_1, \lambda_2, \ldots, \lambda_d, 0, 0, \ldots, 0)$. Thus $\tilde{\Sigma}_d^\dagger = \mathrm{diag}(1/\lambda_1, 1/\lambda_2, \ldots, 1/\lambda_d, 0, 0, \ldots, 0)$ and $\delta^\dagger \tilde{\Sigma}_d^\dagger \delta = 0$.
562 Therefore, $C(F_0^{(B)}, F_1^{(B)}) = 0$.

On the other hand, we have

$$C(F_0^{(A)}, F_1^{(A)}) = \frac{(\delta^\top (I - U_{d-1}U_{d-1}^\top)\delta)^2}{\delta^\top (\Sigma - \Sigma_{d-1})\delta} + \delta^\top \Sigma_{d-1}^\dagger \delta = \frac{s^4}{s^2 \lambda_p} + 0 = s^2/\lambda_p.$$

We can generalize the previous example as follows. Let Σ be a $p \times p$ covariance matrix of the form

$$\Sigma = \begin{bmatrix} \Sigma_d & 0 \\ 0 & \Sigma_d^\perp \end{bmatrix}$$

where Σ_d is a $d \times d$ matrix. Let $\lambda_1 \geq \lambda_2 \geq \cdots \geq \lambda_p$ be the eigenvalues of Σ and suppose furthermore that the
eigenvalues of Σ_d are $\lambda_1, \lambda_2, \ldots, \lambda_d$. Let $\gamma = \lambda_d - \lambda_{d+1}$. We now assume that δ are generated randomly as
follows. The entries of δ are i.i.d. random variable sampled according to the following distribution. Given an
index i, with probability ϵ, $\delta_i = 0$ and with probability $1 - \epsilon$, δ_i is distributed according to a normal distribution
with mean $\tau > 0$ and variance σ^2. Then with probability at least ϵ^d, the covariance matrix for $\tilde{\Sigma}$ is of the form

$$\tilde{\Sigma} = \begin{bmatrix} \Sigma_d & 0 \\ 0 & \Sigma_d^\perp + \frac{1}{4}(\tilde{\delta}\tilde{\delta}^\top) \end{bmatrix}$$

where $\tilde{\delta} \in \mathbb{R}^{p-d}$ is formed by excluding the first d elements of δ. Now, if $\lambda_{d+1} + \frac{1}{4}\|\tilde{\delta}\|^2 < \lambda_d$, then the d largest
eigenvalues of $\tilde{\Sigma}$ is still $\lambda_1, \lambda_2, \ldots, \lambda_d$, and thus the eigenvectors corresponding to the d largest eigenvalues
of $\tilde{\Sigma}$ is the same as that for the d largest eigenvalues of Σ. That is to say,

$$\lambda_{d+1} + \tfrac{1}{4}\|\tilde{\delta}\|^2 < \lambda_d \implies \tilde{\Sigma}_d^\dagger = \Sigma_d^\dagger \implies \delta^\top \tilde{\Sigma}_d^\dagger \delta = 0 \implies C(F_0^{(B)}, F_1^{(B)}) = 0.$$

We now compute the probability that $\lambda_{d+1} + \frac{1}{4}\|\tilde{\delta}\|^2 < \lambda_d$. Suppose for the moment that $\epsilon > 0$ is fixed and
do not varies with p. We then have

$$\frac{\sum_{i=d+1}^p \delta_i^2 - (p-d)(1-\epsilon)\tau^2}{\sqrt{(p-d)(2(1-\epsilon)(2\tau^2\sigma^2 + \sigma^4) + \epsilon(1-\epsilon)(\tau^4 + 2\tau^2\sigma^2 + \sigma^4))}} \xrightarrow{d} N(0,1).$$

Thus, as $p \to \infty$, the probability that $\lambda_{d+1} + \frac{1}{4}\|\tilde{\delta}\|^2 < \lambda_d$ converges to that of

$$\Phi\Big(\frac{4(\lambda_d - \lambda_{d+1}) - (p-d)(1-\epsilon)\tau^2}{\sqrt{(p-d)(2(1-\epsilon)(2\tau^2\sigma^2 + \sigma^4) + \epsilon(1-\epsilon)(\tau^4 + 2\tau^2\sigma^2 + \sigma^4))}} \Big).$$

This probability can be made arbitrarily close to 1 provided that $\lambda_d - \lambda_{d+1} \geq Cp(1 - \epsilon)\tau^2$ for all sufficiently large p and for some constant $C > 1/4$. Since the probability that $\delta_1 = \delta_2 = \cdots = \delta_d$ is at least ϵ^d, we thus conclude that for sufficiently large p, with probability at least ϵ^d,

$$C(F_0^{(B)}, F_1^{(B)}) = 0 < C(F_0^{(A)}, F_1^{(A)}).$$

In the case where $\epsilon = \epsilon(p) \to 1$ as $p \to \infty$ such that $p(1 - \epsilon) \to \theta$ for some constant K, then the probability that $\lambda_{d+1} + \frac{1}{4}\|\tilde{\delta}\|^2 < \lambda_d$ converges to the probability that

$$\frac{1}{4}\sum_{i=1}^{K} \sigma^2 \chi_1^2(\tau) \geq \lambda_d - \lambda_{d+1}$$

where K is Poisson distributed with mean parameter θ and $\chi_i^2(\tau)$ is the non-central chi-square distribution with one degree of freedom and non-centrality parameter τ. Thus if $\lambda_d - \lambda_{d+1} \geq C\theta\tau^2 \log p$ for sufficiently large p and for some constant C, then this probability can also be made arbitrarily close to 1.

IV.E Finite Sample Performance

We now consider the finite sample performance of $\mathtt{LoL}$ and PCA-based classifiers in the high-dimensional setting with small or moderate sample sizes, e.g., when p is comparable to n or when $p \gg n$. Once again we assume that $X|Y = i \sim \mathcal{N}(\mu_i, \Sigma)$ for $i = 0, 1$. Furthermore, we also assume that Σ belongs to the class $\Theta(p, r, k, \tau, \lambda)$ as defined below.

Definition Let $\lambda > 0$, $\tau \geq 1$ and $k \leq p$ be given. Denote by $\Theta(p, r, k, \tau, \lambda, \sigma^2)$ the collection of matrices Σ such that

$$\Sigma = V\Lambda V^\top + \sigma^2 I$$

where V is a $p \times r$ matrix with orthonormal columns and Λ is a $r \times r$ diagonal matrix whose diagonal entries $\lambda_1, \lambda_2, \ldots, \lambda_r$ satisfy $\lambda \geq \lambda_1 \geq \lambda_2 \geq \cdots \geq \lambda_r \geq \lambda/\tau$. In addition, assume also that $|\mathrm{supp}(V)| \leq k$ where $\mathrm{supp}(V)$ denote the non-zero rows of V, i.e., $\mathrm{supp}(V)$ is the subset of $\{1, 2, \ldots, p\}$ such that $V_j \neq 0$ if and only if $j \in \mathrm{supp}(V)$.

We note that in general $r \leq k \ll p$ and $\lambda/\tau \gg \sigma^2$. We then have the following result.

Theorem [37] Suppose there exists constants M_0 and M_1 such that $M_1 \log p \geq \log n \geq M_0 \log \lambda$. Then there exists a constant $c_0 = c_0(M_0, M_1)$ depending on M_0 and M_1 such that for all n and p for which

$$\frac{\tau k}{n} \log \frac{ep}{k} \leq c_0,$$

there exists an estimate $\hat{V}$ of V such that

$$\sup_{\Sigma \in \Theta(p,r,k,\tau,\lambda,\sigma^2)} \mathbb{E}\|\hat{V}\hat{V}^\top - VV^\top\|^2 \leq \frac{Ck(\sigma\lambda + \sigma^2)}{n\lambda^2} \log \frac{ep}{k}$$

where C is a universal constant not depending on p, r, k, τ, λ and σ^2.

We can therefore show that provided that M_0 and M_1 is large enough, and n and p satisfies the condition in the preceding theorem, then provided that the Chernoff information of the population version of $\mathtt{LoL}$ is larger than the Chernoff information of the population version of PCA, the expected Chernoff information for the sample version of $\mathtt{LoL}$ is also larger than the expected Chernoff information of the sample version of PCA. We emphasize that it is necessary that the $\mathtt{LoL}$ and the PCA version both projected into the top $d \leq r$ dimension of the sample covariance matrices.

E   The R implementation of LOL

Figure 8 shows the R implementation of $\mathrm{L_oL}$ for binary classification using FlashMatrix [20]. The implementation takes a $D \times I$ matrix, where each column is a training instance and each instance has D features, and outputs a $D \times k$ projection matrix.

```
\Lol~<- function (m, labels, k) {
        counts <- fm.table(labels)
        num.labels <- length(counts$val)
        num.features <- dim(m)[1]
        nv <- k - (num.labels - 1)
        gr.sum <- fm.groupby(m, 1, fm.as.factor(labels, 2), fm.bo.add)
        gr.mean <- fm.mapply.row(gr.sum, counts$Freq, fm.bo.div, FALSE)
        diff <- fm.get.cols(gr.mean, 1) - fm.get.cols(gr.mean, 2)
        svd <- fm.svd(m, nv=0, nu=nv)
        fm.cbind(diff, svd$u)
}
```

Figure 8: The R implementation of LOL.

F Bibliography

[1] R. A. Fisher, "Theory of Statistical Estimation," *Mathematical Proceedings of the Cambridge Philosophical Society*, vol. 22, no. 05, pp. 700–725, Oct. 1925. [Online]. Available: http://journals.cambridge.org/abstract_S0305004100009580

[2] H. Zou, "The Adaptive Lasso and Its Oracle Properties," pp. 1418–1429, 2006.

[3] Y. LeCun, C. Cortes, and C. Burges, "MNIST handwritten digit database." [Online]. Available: http://yann.lecun.com/exdb/mnist/

[4] P. J. Bickel and E. Levina, "Some theory for Fisher's linear discriminant function, 'naive Bayes', and some alternatives when there are many more variables than observations," *Bernoulli*, vol. 10, no. 6, pp. 989–1010, Dec. 2004. [Online]. Available: http://projecteuclid.org/euclid.bj/1106314847

[5] K.-C. Li, "Sliced Inverse Regression for Dimension Reduction," *Journal of the American Statistical Association*, vol. 86, no. 414, pp. 316–327, Jun. 1991. [Online]. Available: http://www.tandfonline.com/doi/abs/10.1080/01621459.1991.10475035

[6] N. Tishby, F. C. Pereira, and W. Bialek, "The information bottleneck method arXiv : physics / 0004057v1 [physics . data-an] 24 Apr 2000," *Neural Computation*, pp. 1–16, 1999.

[7] A. Globerson and N. Tishby, "Sufficient Dimensionality Reduction," *Journal of Machine Learning Research*, vol. 3, no. 7-8, pp. 1307–1331, Oct. 2003. [Online]. Available: http://www.crossref.org/jmlr_DOI.html

[8] R. D. Cook and L. Ni, "Sufficient Dimension Reduction via Inverse Regression," *Journal of the American Statistical Association*, vol. 100, no. 470, pp. 410–428, Jun. 2005. [Online]. Available: http://amstat.tandfonline.com/doi/abs/10.1198/016214504000001501#.U6tH3Y1dUts

[9] K. Fukumizu, F. R. Bach, and M. I. Jordan, "Dimensionality Reduction for Supervised Learning with Reproducing Kernel Hilbert Spaces," *Journal of Machine Learning Research*, vol. 5, pp. 73–99, 2004.

[10] J. Fan, Y. Feng, and X. Tong, "A road to classification in high dimensional space: the regularized optimal affine discriminant," *Journal of the Royal Statistical Society: Series B (Statistical Methodology)*, vol. 74, no. 4, pp. 745–771, Sep. 2012. [Online]. Available: http://doi.wiley.com/10.1111/j.1467-9868.2012.01029.x

[11] J. Baik and J. W. Silverstein, "Eigenvalues of large sample covariance matrices of spiked population models," *Journal of Multivariate Analysis*, vol. 97, no. 6, pp. 1382–1408, 2006.

[12] D. Paul, "Asymptotics of sample eigenstructure for a large dimensional spiked covariance model," *Statistica Sinica*, vol. 17, no. 4, p. 1617, 2007. [Online]. Available: http://www3.stat.sinica.edu.tw/statistica/oldpdf/A17n418.pdf

[13] T. Hastie, R. Tibshirani, and J. H. Friedman, "The Elements of Statistical Learning: Data Mining, Inference, and Prediction," *BeiJing: Publishing House of Electronics Industry*, 2004.

[14] P. J. Huber, *Robust Statistics*, ser. Wiley Series in Probability and Statistics. Wiley, 1981, vol. 82, no. 3. [Online]. Available: http://doi.wiley.com/10.1002/9780470434697

[15] P. J. Rousseeuw and K. V. Driessen, "A Fast Algorithm for the Minimum Covariance Determinant Estimator," *Technometrics*, vol. 41, no. 3, pp. 212–223, Mar. 1999. [Online]. Available: http://amstat.tandfonline.com/doi/abs/10.1080/00401706.1999.10485670#.VTejtq1Viko

[16] D. Ferrari and Y. Yang, "Maximum L q -likelihood estimation," *The Annals of Statistics*, vol. 38, no. 2, pp. 753–783, apr 2010. [Online]. Available: http://projecteuclid.org/euclid.aos/1266586613

[17] E. J. Candès, X. Li, Y. Ma, and J. Wright, "Robust Principal Component Analysis?" *Journal of the ACM*, vol. 58, no. 3, pp. 1–37, Dec. 2009. [Online]. Available: http://dl.acm.org/citation.cfm?id=1970392.1970395http://arxiv.org/abs/0912.3599

[18] T. Zhang and G. Lerman, "A Novel M-Estimator for Robust PCA," *Journal of Machine Learning Research*, vol. 15, pp. 749–808, 2014. [Online]. Available: http://jmlr.org/papers/v15/zhang14a.html

[19] C. M. Bishop, *Pattern Recognition and Machine Learning*, ser. Information science and statistics. Springer, 2006. [Online]. Available: http://www.library.wisc.edu/selectedtocs/bg0137.pdf

[20] D. Zheng, D. Mhembere, J. T. Vogelstein, C. E. Priebe, and R. Burns, "Flashmatrix: Parallel, scalable data analysis with generalized matrix operations using commodity ssds," *arXiv preprint arXiv:1604.06414*, 2016.

[21] D. Zheng, D. Mhembere, R. Burns, J. Vogelstein, C. E. Priebe, and A. S. Szalay, "FlashGraph: Processing billion-node graphs on an array of commodity SSDs," in *13th USENIX Conference on File and Storage Technologies (FAST 15)*, Santa Clara, CA, 2015.

[22] D. Zheng, R. Burns, J. Vogelstein, C. E. Priebe, and A. S. Szalay, "An ssd-based eigensolver for spectral analysis on billion-node graphs," *CoRR*, vol. abs/1602.01421, 2016.

[23] D. Zheng, D. Mhembere, V. Lyzinski, J. Vogelstein, C. E. Priebe, and R. Burns, "Semi-external memory sparse matrix multiplication on billion-node graphs in a multicore architecture," *CoRR*, vol. abs/1602.02864, 2016.

[24] G. M. Amdahl, "Validity of the Single Processor Approach to Achieving Large Scale Computing Capabilities," in *AFIPS Spring Joint Computer Conference, 1967. AFIPS '67 (Spring). Proceedings of the*, vol. 30, 1967, pp. 483–485. [Online]. Available: http://delivery.acm.org/10.1145/1470000/ 1465560/p483-amdahl.pdf?ip=202.189.127.238{&}id=1465560{&}acc=ACTIVESERVICE{&}key= CDD1E79C27AC4E65.DE0A32330AE3471B.4D4702B0C3E38B35.4D4702B0C3E38B35{&}CFID= 646862329{&}CFTOKEN=33418015{&}{_}{_}acm{_}{_}=1426882996{_}a666a43ab4250317fe0

[25] J. Abello, A. L. Buchsbaum, and J. R. Westbrook, "A functional approach to external graph algorithms," in *AlgorithmsESA98*. Springer, 1998, pp. 332–343.

[26] E. J. Candès and T. Tao, "Near-Optimal Signal Recovery From Random Projections: Universal Encoding Strategies?" *IEEE Transactions on Information Theory*, vol. 52, no. 12, pp. 5406–5425, dec 2006. [Online]. Available: http://ieeexplore.ieee.org/lpdocs/epic03/wrapper.htm?arnumber=4016283

[27] T. Hastie, K. W. Church, P. Li, and K. C. Kdd, "Very sparse random projections," *Proceedings of the 12th ACM SIGKDD international conference on Knowledge discovery and data mining - KDD '06*, p. 287, 2006. [Online]. Available: http://portal.acm.org/citation.cfm?doid=1150402.1150436

[28] M. Lopes, L. Jacob, and M. J. Wainwright, "A More Powerful Two-Sample Test in High Dimensions using Random Projection," in *Neural Information Processing Systems*, 2011, pp. 1206–1214. [Online]. Available: http://papers.nips.cc/paper/ 4260-a-more-powerful-two-sample-test-in-high-dimensions-using-random-projection

[29] P. N. Belhumeur, J. P. Hespanha, and D. J. Kriegman, "Eigenfaces vs. fisherfaces: Recognition using class specific linear projection," *IEEE Transactions on Pattern Analysis and Machine Intelligence*, vol. 19, no. 7, pp. 711–720, 1997.

[30] S. Mika, G. Ratsch, J. Weston, B. Scholkopf, and K. Mullers, "Fisher discriminant analysis with kernels," in *Neural Networks for Signal Processing IX: Proceedings of the 1999 IEEE Signal Processing Society Workshop (Cat. No.98TH8468)*. IEEE, 1999, pp. 41–48. [Online]. Available: http://ieeexplore.ieee.org/lpdocs/epic03/wrapper.htm?arnumber=788121

[31] L. Breiman, "Random forests," *Machine learning*, vol. 45, no. 1, pp. 5–32, 2001.

[32] W. K. Allard, G. Chen, and M. Maggioni, "Multi-scale geometric methods for data sets II: Geometric Multi-Resolution Analysis," *Applied and Computational Harmonic Analysis*, vol. 32, no. 3, pp. 435–462, May 2012. [Online]. Available: http://linkinghub.elsevier.com/retrieve/pii/S1063520311000868

[33] E. Anderson, Z. Bai, C. Bischof, S. Blackford, J. Demmel, J. Dongarra, J. D. Croz, A. Greenbaum, S. Hammerling, A. McKenney, and D. Sorensen, *LAPACK Users' Guide: Third Edition.* SIAM, 1999. [Online]. Available: https://books.google.com/books?hl=en&lr=&id=AZlvEnr9gCgC&pgis=1

[34] H. Chernoff, "A measure of asymptotic efficiency for tests of a hypothesis based on the sum of observations," *Annals of Mathematical Statistics*, vol. 23, pp. 493–507, 1952.

[35] I. Csizár, "Information-type measures of difference of probability distributions and indirect observations," *Studia Scientiarum Mathematicarum Hungarica*, vol. 2, pp. 229–318, 1967.

[36] C. C. Leang and D. H. Johnson, "On the asymptotics of M-hypothesis bayesian detection," *IEEE Transactions on Information Theory*, vol. 43, pp. 280–282, 1997.

[37] T. T. Cai, Z. Ma, and Y. Wu, "Optimal estimation and rank detection for sparse spiked covariance matrices," 2013, arxiv preprint at http://arxiv.org/abs/1305.3235.